

TRAMP: Compositional Inference with TRee Approximate Message Passing

Antoine Baker¹, Benjamin Aubin², Florent Krzakala¹, and Lenka Zdeborová²

¹Laboratoire de Physique, CNRS, École Normale Supérieure, PSL University, Paris, France

²Institut de Physique Théorique, CNRS, CEA, Université Paris-Saclay, Saclay, France

June 26, 2022

Abstract

We introduce *tramp*, standing for *TRee Approximate Message Passing*, a python package for compositional inference in high-dimensional tree-structured models. The package provides a unifying framework to study several approximate message passing algorithms previously derived for a variety of machine learning tasks such as generalized linear models, inference in multi-layer networks, matrix factorization, and reconstruction using non-separable penalties. For some models, the asymptotic performance of the algorithm can be theoretically predicted by the state evolution, and the measurements entropy estimated by the free entropy formalism. The implementation is modular by design: each module, which implements a factor, can be composed at will with other modules to solve complex inference tasks. The user only needs to declare the factor graph of the model: the inference algorithm, state evolution and entropy estimation are fully automated. The source code is publicly available at <https://github.com/sphinxteam/tramp>.

Contents

1	Introduction	4
2	Expectation Propagation	6
2.1	Bethe free energy	6
2.2	Weak consistency	7
2.3	Moments and natural parameters duality	8
2.4	Graph decomposition of the free energy	8
2.5	Tramp implementation of Expectation Propagation	9
2.6	Expectation Propagation modules	10
2.7	Related algorithms	11
2.8	EP, EC, AdaTAP and Message-Passing	14
3	State evolution	14
3.1	Setting	14
3.2	Ensemble average at fixed precisions	15
3.3	Tramp implementation of state evolution	16
3.4	Expression in term of mutual information	17
3.5	Duality between overlaps/variances and precisions	17
3.6	Graph decomposition of the free entropy	18
3.7	State evolution modules	19
4	Examples	19
4.1	Benchmark on sparse linear regression	19
4.2	Depicting tramp modularity	20
4.2.1	Sparse DFT/gradient denoising	21
4.2.2	Variational Auto-Encoder on MNIST	21
4.3	Theoretical prediction of performance	23
5	Discussion	24
A	Proof of Proposition 1	26
A.1	Minimization of $G[\{\mu_x\}]$	26
A.2	Stationary point of $A[\{\lambda_x, \lambda_f\}]$	27
A.3	Stationary point of $A[\{\lambda_{x \rightarrow f}, \lambda_{f \rightarrow x}\}]$	27
B	Tramp modules	28
B.1	Variable	28
B.1.1	General variable	28
B.1.2	Isotropic Gaussian variable	28
B.1.3	Diagonal Gaussian variable	28
B.1.4	Full covariance Gaussian variable	29
B.1.5	Real variable	29
B.1.6	Binary variable	29
B.1.7	Sparse variable	29
B.1.8	Interval variable	30
B.1.9	Positive/negative variable	30
B.1.10	Phase (circular) variable	30
B.2	Linear channels	31
B.2.1	Generic linear channel	31
B.2.2	Ensemble average	31
B.2.3	Random matrix theory expressions	31
B.2.4	Rotation channel	32
B.2.5	Scaling channel	32

B.2.6	SVD decomposition	33
B.2.7	Complex linear channel	33
B.2.8	Unitary channel	33
B.2.9	Convolution channel (complex)	33
B.2.10	Convolution channel (real)	33
B.2.11	Full covariance beliefs	34
B.3	Separable priors	34
B.3.1	Generic separable prior	34
B.3.2	Ensemble average	35
B.3.3	Natural prior	35
B.3.4	Gaussian prior	36
B.3.5	Binary prior	36
B.3.6	Sparse prior	37
B.3.7	Interval prior	37
B.4	Separable likelihoods	37
B.4.1	Generic separable likelihood	37
B.4.2	Ensemble average	38
B.4.3	Gaussian likelihood	38
B.4.4	Sgn likelihood	39
B.4.5	Abs likelihood	39
B.4.6	Phase likelihood	39
B.4.7	Modulus likelihood	40
B.5	Separable channels	40
B.5.1	Generic separable channel	40
B.5.2	Ensemble average	40
B.5.3	Gaussian noise channel	41
B.5.4	Piecewise linear activation	42
C	Proof of overlap/variance precision duality	43
C.1	Derivative of A_x and I_x	43
C.2	Derivative of A_f and I_f	43
D	Proof of Proposition 3	44
D.1	Minimization of $A^*[\{m_x\}]$	44
D.2	Stationary point of $A[\{a_x, a_f\}]$	44
D.3	Stationary point of $A[\{a_{x \rightarrow f}, a_{f \rightarrow x}\}]$	44

1 Introduction

Probabilistic models have been used in many applications, as diverse as scientific data analysis, coding, natural language and signal processing. It also offers a powerful framework [Bishop, 2013] to several challenges in machine learning: dealing with uncertainty, choosing hyper-parameters, causal reasoning and model selection. However, the difficulty of deriving and implementing approximate inference algorithms for each new model may have hindered the wider adoption of Bayesian methods. The probabilistic programming approach seeks to make Bayesian inference as user friendly and streamlined as possible: ideally the user would only need to declare the probabilistic model and run an inference engine. Several probabilistic programming frameworks have been proposed, well suited for different contexts and leveraging variational inference or sampling methods to automate inference. To give a few examples, pomegranate [Schreiber, 2018] fits probabilistic models using maximum likelihood. Church [Goodman et al., 2008] and successors are universal languages for representing generative models. Infer.NET [Minka et al., 2018] implements several message passing algorithms such as Expectation Propagation. Stan [Carpenter et al., 2017] uses Hamiltonian Monte Carlo, while Anglican [Wood et al., 2014] uses particle MCMC as the sampling method. Turing [Ge et al., 2018] offers a Julia implementation. Recently, Edward [Tran et al., 2016] and Pyro [Bingham et al., 2018] tackle deep probabilistic problems, scaling inference up to large data and complex models.

In this paper, we present tramp (TRee Approximate Message Passing). In the current rich software ecosystem, tramp aims to fill a particular niche: using message passing-algorithms with theoretical guarantees of performance in specific asymptotic settings. As an alternative to tramp let us mention the **vampyre** package that allows inference in multi-layer networks [Fletcher et al., 2018].

There is a long history behind message passing [Yedidia and Freeman, 2001, Mezard and Montanari, 2009], approximate message passing (AMP) [Donoho et al., 2009] and vector approximate message passing (VAMP) [Schniter et al., 2017], that we shall discuss later on. As exemplified in the context of compressed sensing, the AMP algorithm has a fundamental property: its performance on random instances in the high-dimensional limit, measured by the mean squared error on the signals, can be rigorously predicted by the so-called state evolution [Donoho et al., 2009, Bayati and Montanari, 2011], a rigorous version of the physicists "cavity method" [Mézarid et al., 1987]. These performances can be shown, in some cases, to reach the Bayes optimal one in polynomial time [Barbier et al., 2016, Reeves and Pfister, 2016], quite a remarkable feat! More recently, variant of the AMP approach has been developed with (some) correlated data and matrices [Schniter et al., 2017, Ma and Ping, 2017], again with guarantees of optimality in some cases [Barbier et al., 2018, Gerbelot et al., 2020]. These approaches are intimately linked with the Expectation Propagation algorithm [Minka, 2001a] and the Expectation Consistency framework [Oppor and Winther, 2005a].

The state evolution and the Bayes optimal guarantees were extended to a wide variety of models including for instance generalized linear models (GLM) [Rangan, 2011, Barbier et al., 2019], matrix factorization [Rangan and Fletcher, 2012, Deshpande and Montanari, 2014, Dia et al., 2016, Lesieur et al., 2017], committee machines [Aubin et al., 2018], optimization with non separable penalties (such as total variation) [Som and Schniter, 2012, Metzler et al., 2015, Tan et al., 2015, Manoel et al., 2018], inference in multi-layer networks [Manoel et al., 2017, Fletcher et al., 2018, Gabrié et al., 2018] and even arbitrary trees of GLMs [Reeves, 2017]. In all these cases, the entropy of the system in the high dimensional limit can be obtained as the minimum of the so-called free entropy potential [Yedidia and Freeman, 2001, Yedidia et al., 2005, Krzakala et al., 2014] and this allows the computation of interesting information theoretic quantities such as the mutual information between layers in a neural network [Gabrié et al., 2018]. Furthermore, the global minimizer of the free entropy potential corresponds to the minimal mean squared error, which allows to determine fundamental limits to inference. Interestingly, the mean squared error achieved by AMP, predicted by the state evolution, is a stationary point of the same free entropy potential, which allows for an interesting interpretation of when the algorithm actually works [Zdeborová and Krzakala, 2016] in terms of phase transitions.

Unfortunately the development of AMP algorithms faced the same caveat as probabilistic modeling: for each new model, the AMP algorithm and the associated theory (free entropy and state evolution) had to be derived and implemented separately, which can be time-consuming. However, a key observation is that the factor graphs [Kschischang et al., 2001] for all the models mentioned above are tree-structured as illustrated in Figure 1. Each factor corresponds to an elementary inference problem that can be solved analytically or approximately. The tramp python package —where tramp stands for tree approximate message passing— offers a unifying framework for all the models discussed above and extends to arbitrary tree-structured models.

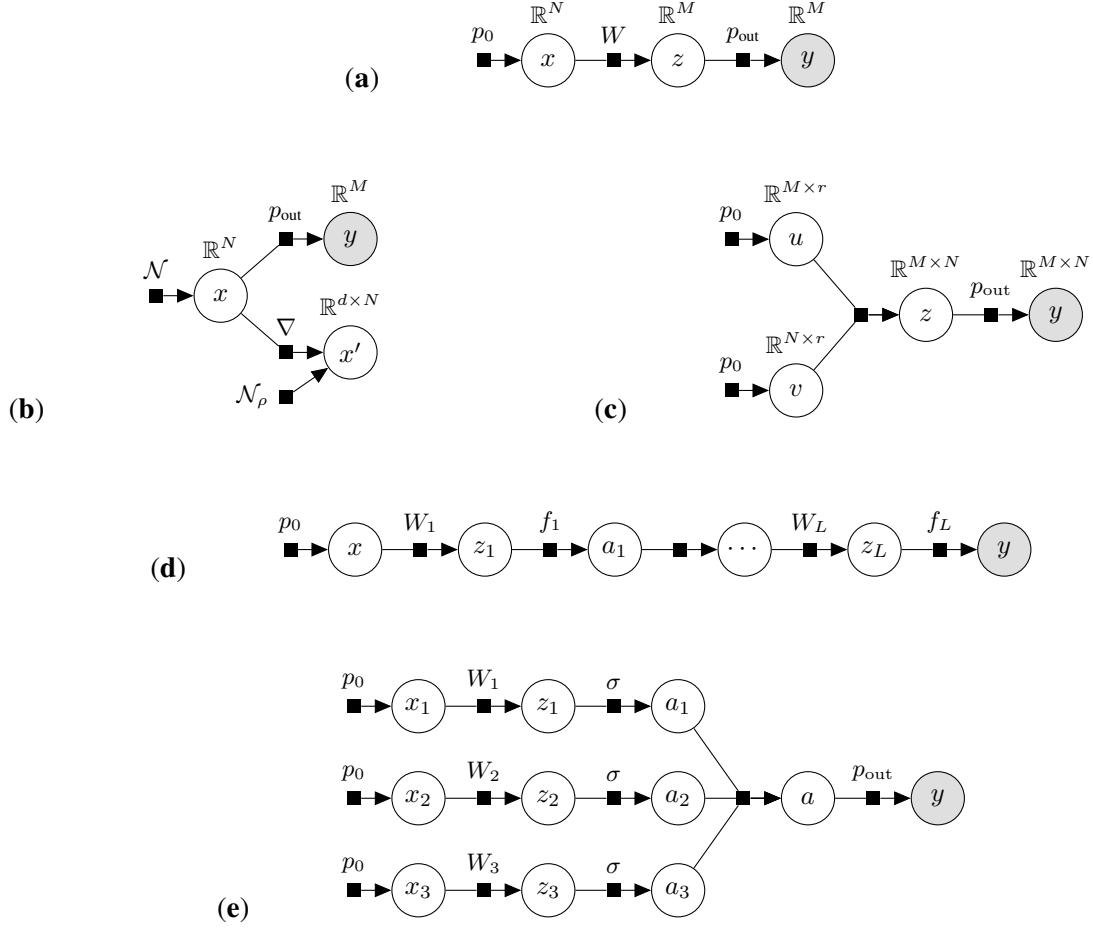


Figure 1: Tree-structured models. **(a)** Generalized linear model with separable prior $p_0(x)$, separable likelihood $p_{\text{out}}(y|z)$ and linear channel $z = Wx$. **(b)** Reconstruction using a sparse gradient prior where sparsity is enforced by the Gauss-Bernoulli prior $\mathcal{N}_\rho = [1 - \rho]\delta + \rho\mathcal{N}$. **(c)** Low-rank matrix factorization with separable priors p_0 , separable likelihood $p_{\text{out}}(y|z)$ and factorization $z = uv^T$. **(d)** Multi-layer network with activation functions $a_l = f_l(z_l)$ and linear channels $z_l = W_l a_{l-1}$. **(e)** Committee machine with three experts.

Similar to other probabilistic programming frameworks, the user only has to declare the model (here a tree-structured factor graph) then the inference, state evolution and entropy estimation are fully automated. The implementation is also completely modularized and extending tramp is in principle straightforward. If a new factor is needed, the user only has to solve (analytically or approximately) the elementary inference problem corresponding to this factor and implement it as a module in tramp. The source code is publicly available at <https://github.com/sphinxsteam/tramp>.

Many of the AMP algorithms previously mentioned, especially the vectorized versions considered in [Schniter et al., 2017, Manoel et al., 2018, Fletcher et al., 2018], can be stated as particular instances of the Expectation Propagation (EP) algorithm [Minka, 2001a, Oppor and Winther, 2005a]. In Section 2 we generalize this approach to arbitrary tree-structured models. This section is mainly a review of the Heskes et al. [2005] derivation of EP as a relaxed variational problem, which allows us to introduce the key quantities (posterior moments and log-evidence) implemented in tramp, where EP is used as the inference engine. Next in Section 3 we show that the state evolution and the free entropy potential can be reinterpreted as simple ensemble average of the posterior variances and log-evidence estimated by EP. This allows us to conjecture how to extend the state evolution and entropy estimation to tree-structured models and implement them in the tramp package. Finally, in Section 4 we illustrate the package on a few examples.

2 Expectation Propagation

In this section we review the derivation of EP as a relaxed variational problem. First we briefly recall the variational inference framework and the Bethe decomposition of the free energy [Yedidia and Freeman, 2001] which is exact for tree-structured models. Then following Heskes et al. [2005], the Bethe variational problem can be approximately solved by enforcing moment-matching instead of full consistency of the marginals, which yields the EP algorithm. The EP solution consists of exponential family distributions which satisfy a duality between natural parameters and moments [Wainwright and Jordan, 2008]. Finally we expose the tramp implementation of EP.

2.1 Bethe free energy

Let's consider a general inference problem $p(\mathbf{x}, \mathbf{y})$ where $\mathbf{x} = \{x\}$ are the signals to infer and $\mathbf{y} = \{y\}$ the measurements. We emphasize that each signal x and measurement y is itself a high dimensional object in the typical cases under consideration (Figure 1). The goal of the inference is to get the posterior $p(\mathbf{x}|\mathbf{y})$ and evidence $p(\mathbf{y})$, or equivalently the negative log-evidence known as surprisal in information theory. We will assume that $p(\mathbf{x}, \mathbf{y})$ can be factorized as a tree-structured probabilistic graphical model (PGM):

$$p(\mathbf{x}, \mathbf{y}) = \frac{1}{Z_0} \prod_f f(x_f; y_f), \quad Z_0 = \int \prod_x dx \prod_y dy \prod_f f(x_f; y_f), \quad (1)$$

where $\{f\}$ is the set of factors of the model, $x_f = \{x \in f\}$ denotes the set of variables of the factor f and $y_f = \{y \in f\}$ denotes the set of measurements attached to the factor f , see Figure 2 for an example. We will sometimes write factors as functions of the variables only $f(x_f) = f(x_f; y_f)$, where the dependence upon the measurements is implicit. For the factorization Eq. (1) the posterior is equal to:

$$p(\mathbf{x}|\mathbf{y}) = \frac{1}{Z(\mathbf{y})} \prod_f f(x_f; y_f), \quad Z(\mathbf{y}) = \int \prod_x dx \prod_f f(x_f; y_f). \quad (2)$$

The *Helmholtz free energy* is here defined as the negative log partition

$$F(\mathbf{y}) = -\ln Z(\mathbf{y}) = -\ln p(\mathbf{y}) - \ln Z_0, \quad (3)$$

and gives the surprisal up to a constant. When the PGM is a Bayesian network, for instance all the models except (b) in Figure 1, the factors are the conditional probabilities $f(x_f; y_f) = p(x_f^+, y_f | x_f^-)$, where x_f^-, x_f^+ denote the subsets of input/output variables attached to the factor f and y_f the measurements (if any) attached to the factor f . In that case, the normalization constant $Z_0 = 1$ and the Helmholtz free energy is directly equal to the surprisal.

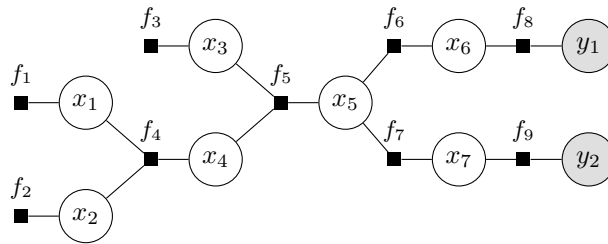


Figure 2: Illustration of a tree-structured PGM with measurements $\mathbf{y} = \{y_1, y_2\}$, signals $\mathbf{x} = \{x_i\}_{i=1}^7$ and factors $\{f_k\}_{k=1}^9$. For this factor graph the variables corresponding to each factor are given by $x_{f_1} = \{x_1\}$, $x_{f_2} = \{x_2\}$, $x_{f_3} = \{x_3\}$, $x_{f_4} = \{x_1, x_2, x_4\}$, $x_{f_5} = \{x_3, x_4, x_5\}$, $x_{f_6} = \{x_5, x_6\}$, $x_{f_7} = \{x_5, x_7\}$, $x_{f_8} = \{x_6\}$ and $x_{f_9} = \{x_7\}$. For the likelihood factors, we denote either implicitly or explicitly the dependence upon the measurements: $f_8(x_6) = f_8(x_6; y_1)$ and $f_9(x_7) = f_9(x_7; y_2)$.

We are interested in computationally hard inference problems and seek an approximation q of the posterior distribution $q(\mathbf{x}) \simeq p(\mathbf{x}|\mathbf{y})$. Consider such an approximation q and the following functional

$$\mathcal{F}[q] = \text{KL}[q(\mathbf{x}) \| p(\mathbf{x}|\mathbf{y})] + F(\mathbf{y}), \quad (4)$$

called the *variational free energy*. As the KL divergence is always positive and equal to zero only if the two distributions are equal, we can formally get the posterior and the Helmholtz free energy $F(\mathbf{y})$ as the solution of the variational problem:

$$F(\mathbf{y}) = \min_q \mathcal{F}[q] \quad \text{for} \quad q^*(\mathbf{x}) = p(\mathbf{x}|\mathbf{y}). \quad (5)$$

However, for a tree-structured PGM we know that the posterior factorizes as

$$p(\mathbf{x}|\mathbf{y}) = \frac{\prod_f p(x_f|\mathbf{y})}{\prod_x p(x|\mathbf{y})^{n_x-1}}, \quad (6)$$

where $p(x|\mathbf{y})$ is the marginal of the variable x , $p(x_f|\mathbf{y})$ is the joint marginal over x_f and n_x is the number of neighbor factors of the variable x . Therefore we can restrict the variational problem Eq. (5) to distributions of the form

$$q(\mathbf{x}) = \frac{\prod_f q_f(x_f)}{\prod_x q_x(x)^{n_x-1}}, \quad (7)$$

and minimize over the set of variable marginals $\{q_x\}$ and factor marginals $\{q_f\}$. Note that the factor and variable marginals have to belong to the set of consistent marginals

$$\mathcal{M} = \left\{ \{q_x, q_f\} : \quad \forall f, \forall x \in f, \quad q_x(x) = \int dx_{f \setminus x} q_f(x_f) \right\}. \quad (8)$$

For distributions of the type Eq. (7), the variational free energy Eq. (4) is equal to

$$\mathcal{F}_{\text{Bethe}}[\{q_f, q_x\}] = \sum_f F_f[q_f] + \sum_x (1 - n_x) F_x[q_x], \quad (9)$$

$$F_f[q_f] = \text{KL}[q_f \| f], \quad F_x[q_x] = -H[q_x], \quad (10)$$

called the *Bethe free energy* [Yedidia and Freeman, 2001], where KL and H denote respectively the Kullback-Leibler divergence and the entropy. Therefore for a tree-structured PGM we have:

$$F(\mathbf{y}) = \min_{\{q_f, q_x\} \in \mathcal{M}} \mathcal{F}_{\text{Bethe}}[\{q_f, q_x\}] \quad \text{for} \quad q^*(\mathbf{x}) = p(\mathbf{x}|\mathbf{y}). \quad (11)$$

The solution of this Bethe variational problem actually leads to the Belief Propagation algorithm [Pearl, 1988, Yedidia and Freeman, 2001].

2.2 Weak consistency

For tree-structured PGMs the Bethe variational problem Eq. (11) yields the exact posterior and Helmholtz free energy, and is solved by the Belief Propagation algorithm. Unfortunately for the PGMs introduced in Figure 1, which involve high-dimensional vectors or matrices, the Belief Propagation algorithm is not tractable. Following Heskes et al. [2005] we consider instead a relaxed version of the Bethe variational problem, by replacing the strong consistency constraint Eq. (8) by the *weak consistency* constraint:

$$\mathcal{M}_\phi = \left\{ \{q_x, q_f\} : \quad \forall f, \forall x \in f, \quad \mathbb{E}_{q_x} \phi(x) = \mathbb{E}_{q_f} \phi(x) \right\}, \quad (12)$$

for a chosen set of sufficient statistics $\{\phi(x)\}$. In other words instead of requiring the full consistency of the marginals, we only require moment matching. The *relaxed Bethe variational problem*:

$$F_\phi(\mathbf{y}) = \min_{\{q_f, q_x\} \in \mathcal{M}_\phi} \mathcal{F}_{\text{Bethe}}[\{q_f, q_x\}] \simeq F(\mathbf{y}) \quad \text{for} \quad q^*(\mathbf{x}) \simeq p(\mathbf{x}|\mathbf{y}), \quad (13)$$

leads to the solution [Heskes et al., 2005]:

$$q_f^*(x_f) = f(x_f) e^{\lambda_f^\top \phi(x_f) - A_f[\lambda_f]}, \quad (14)$$

$$q_x^*(x) = e^{\lambda_x^\top \phi(x) - A_x[\lambda_x]}, \quad (15)$$

$$\lambda_f = \{\lambda_{x \rightarrow f}\}_{x \in f}, \quad (16)$$

$$(n_x - 1)\lambda_x = \sum_{f \in x} \lambda_{x \rightarrow f}, \quad (17)$$

$$\mu_x^* = \mu_x[\lambda_x] = \mu_x^f[\lambda_f], \quad (18)$$

where $\mu_x[\lambda_x] = \mathbb{E}_{q_x^*} \phi(x)$ and $\mu_x^f[\lambda_f] = \mathbb{E}_{q_f^*} \phi(x)$ are the moments of the variable x as estimated by the variable and factor marginal respectively. This is the fixed point searched by the EP algorithm [Minka, 2001a].

2.3 Moments and natural parameters duality

The factor marginal q_f and variable marginal q_x are both in the exponential family, with associated natural parameters λ_f and λ_x . The log-partitions

$$A_f[\lambda_f] = \ln \int dx_f f(x_f) e^{\lambda_f^\top \phi(x_f)}, \quad (19)$$

$$A_x[\lambda_x] = \ln \int dx e^{\lambda_x^\top \phi(x)}, \quad (20)$$

are convex functions and provide the bijective mappings between the convex set of natural parameters and the convex set of moments [Wainwright and Jordan, 2008]:

$$\mu_f[\lambda_f] = \mathbb{E}_{q_f} \phi(x_f) = \partial_{\lambda_f} A_f[\lambda_f], \quad (21)$$

$$\mu_x[\lambda_x] = \mathbb{E}_{q_x} \phi(x) = \partial_{\lambda_x} A_x[\lambda_x], \quad (22)$$

and the inverse mappings are given by:

$$\lambda_f[\mu_f] = \partial_{\mu_f} G_f[\mu_f], \quad (23)$$

$$\lambda_x[\mu_x] = \partial_{\mu_x} G_x[\mu_x], \quad (24)$$

where $G_x[\mu_x] = \max_{\lambda_x} \lambda_x^\top \mu_x - A_x[\lambda_x]$ and $G_f[\mu_f] = \max_{\lambda_f} \lambda_f^\top \mu_f - A_f[\lambda_f]$ are the Legendre transformations (convex conjugates) of the log-partitions and are equal to the KL divergence and the negative entropy respectively:

$$G_f[\mu_f] = \text{KL}[q_f \| f], \quad (25)$$

$$G_x[\mu_x] = -H[q_x]. \quad (26)$$

2.4 Graph decomposition of the free energy

Let's introduce the Gibbs free energy [Oppor and Winther, 2005b] and the Minka [2001b] free energy:

$$G[\{\mu_x\}] = \sum_f G_f[\mu_f] + \sum_x (1 - n_x) G_x[\mu_x] \quad (27)$$

$$A[\{\lambda_x, \lambda_f\}] = \sum_f A_f[\lambda_f] + \sum_x (1 - n_x) A_x[\lambda_x]. \quad (28)$$

The Gibbs free energy is a function over the posterior moments with $\mu_f = \{\mu_x\}_{x \in f}$ while the Minka free energy is a function over the variable and factor natural parameters. The tramp free energy is the same as the Minka free energy but is parametrized in term of factor to variable messages $\lambda_{f \rightarrow x}$ and variable to factor messages $\lambda_{x \rightarrow f}$:

$$A[\{\lambda_{f \rightarrow x}, \lambda_{x \rightarrow f}\}] = \sum_f A_f[\lambda_f] - \sum_{x \in f} A_x[\lambda_x^f] + \sum_x A_x[\lambda_x], \quad (29)$$

$$\lambda_f = \bigcup_{x \in f} \lambda_{x \rightarrow f}, \quad \lambda_x^f = \lambda_{x \rightarrow f} + \lambda_{f \rightarrow x}, \quad \lambda_x = \sum_{f \in x} \lambda_{f \rightarrow x}. \quad (30)$$

The parametrization Eq. (30) in term of messages has a nice interpretation: the variable natural parameter is the sum of the incoming messages (coming from the neighboring factors), the factor natural parameter is the union of the incoming messages (coming from the neighboring variables).

Proposition 1 *The relaxed Bethe variational problem Eq. (13) can be formulated in term of the posterior moments using the Gibbs free energy, in term of the factor and variable natural parameters using the Minka free energy, or in term of the natural parameters messages using the tramp free energy:*

$$F_\phi(\mathbf{y}) = \min_{\{\mu_x\}} G[\{\mu_x\}] \quad (31)$$

$$= \min_{\{\lambda_x\}} \max_{\{\lambda_f\}} -A[\{\lambda_x, \lambda_f\}] \quad \text{s.t.} \quad (n_x - 1)\lambda_x = \sum_{f \in x} \lambda_{x \rightarrow f} \quad (32)$$

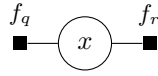
$$= \min_{\{\lambda_{f \rightarrow x}, \lambda_{x \rightarrow f}\}} \text{extr} -A[\{\lambda_{f \rightarrow x}, \lambda_{x \rightarrow f}\}]. \quad (33)$$

Besides, any stationary point of the free energies (not necessarily the global optima) is an EP fixed point:

$$\mu_x = \mu_x^f, \quad (n_x - 1)\lambda_x = \sum_{f \in x} \lambda_{x \rightarrow f}. \quad (34)$$

See [Minka, 2001b, Heskes et al., 2005, Wainwright and Jordan, 2008] for separate derivations of these equivalences or Appendix A for a condensed proof. Note that the Bethe, Gibbs, Minka and tramp free energies all follow the same graph decomposition: a sum over factors – sum over edges + sum over variables. The same graph decomposition holds for the Helmholtz free energy $F(\mathbf{y})$ and the EP approximation $F_\phi(\mathbf{y})$. Indeed $F(\mathbf{y})$ is simply the Bethe free energy evaluated at the true marginals according to Eq. (11) and $F_\phi(\mathbf{y})$ is the Minka/Gibbs/tramp free energy evaluated at the optimal EP fixed point according to Proposition 1.

Remark 2 The above Proposition 1 is closely related to the Expectation Consistency (EC) framework [Oppen and Winther, 2005a,b]. The EC approximation for the log-partition exactly corresponds to the Minka free energy A for a very simple factor graph with only one variable x and two factors $f_q(x)$ and $f_r(x)$. The denomination "Gibbs free energy" for G the dual of A is actually coined from this work.



The EC approximation can be straightforwardly generalized to any tree-structured factor graph, which yields another equivalent derivation of Proposition 1.

2.5 Tramp implementation of Expectation Propagation

The tramp implementation of EP works with the full set of messages $\{\lambda_{f \rightarrow x}, \lambda_{x \rightarrow f}\}$. A stationary point of $A[\{\lambda_{f \rightarrow x}, \lambda_{x \rightarrow f}\}]$ satisfies:

$$\partial_{\lambda_{f \rightarrow x}} A = 0 \iff \mu_x[\lambda_x^f] = \mu_x[\lambda_x] \iff \lambda_x^f = \lambda_x, \quad (35)$$

$$\partial_{\lambda_{x \rightarrow f}} A = 0 \iff \mu_x[\lambda_x^f] = \mu_x^f[\lambda_f] \iff \lambda_x^f = \lambda_x[\mu_x^f[\lambda_f]], \quad (36)$$

which suggests the iterative procedure summarized in Algorithm 1, where E_+ denotes a topological ordering of the edges and E_- the reverse ordering.

The message-passing schedule seems the most natural: iterate over the edges in topological order (forward pass) then iterate in reverse topological order (backward pass) and repeat until convergence. In fact, if the exponential beliefs and the factors are conjugate¹ then the moment-matching is exact and Algorithm 1 is actually equivalent to exact belief propagation, where one forward pass and one backward pass yield the exact marginals [Bishop, 2006].

Algorithm 1: Expectation Propagation in tramp

input: observations $\{y\}$

output: posterior natural parameters $\{\lambda_x\}$

initialize $\lambda_{x \rightarrow f}, \lambda_{f \rightarrow x} = 0$

repeat

foreach edge $e \in E_+ \cup E_-$ **do**

 // forward and backward pass

if $e = f \rightarrow x$ **then**

$\lambda_x^f = \lambda_x[\mu_x^f[\lambda_f]]$

 // moment-matching

$\lambda_{f \rightarrow x}^{\text{new}} = \lambda_x^f - \lambda_{x \rightarrow f}$

 // message $f \rightarrow x$

if $e = x \rightarrow f$ **then**

$\lambda_x = \sum_{g \in x} \lambda_{g \rightarrow x}$

 // posterior

$\lambda_{x \rightarrow f}^{\text{new}} = \lambda_x - \lambda_{f \rightarrow x}$

 // message $x \rightarrow f$

until convergence

¹For example Gaussian beliefs and the factors are either linear transform or Gaussian noise, prior or likelihood

2.6 Expectation Propagation modules

We have the freedom to choose any kind of approximate beliefs, that is choose a set of sufficient statistics $\phi(x)$ for each variable x . Each choice leads to a different approximate inference scheme, but all are implemented by the same message passing Algorithm 1. Of course the algorithm requires each relevant module to be implemented: in practice the variable x (resp. factor f) module should be able to compute the log-partition $A_x[\lambda_x]$ (resp. $A_f[\lambda_f]$) and its associated moment function $\mu_x[\lambda_x]$ (resp. $\mu_f[\lambda_f]$). Note that the definition of the module directly depends on the choice of sufficient statistics $\phi(x)$, so choosing a different kind of approximate beliefs actually leads to a distinct module. We list below the modules considered in tramp.

Variable modules A list of approximate beliefs is presented in Appendix B.1. As shown, such beliefs can be defined over many types of variable: binary, sparse, real, constrained to an interval, or circular for instance. The associated variable modules correspond to well known exponential family distributions, including the Gauss-Bernoulli for a sparse variable.

Isotropic Gaussian beliefs Currently the tramp package only implements isotropic Gaussian beliefs on each variable $x \in \mathbb{R}^{N_x}$, that is we choose $\phi(x) = \{x, -\frac{1}{2}x^\top x\}$ as sufficient statistics, the associated natural parameters are $b_x \in \mathbb{R}^{N_x}$ (a vector of same dimension as x) and the scalar precision $a_x \in \mathbb{R}$. The log-partition, mean r_x and variance v_x for the variable marginal are equal to

$$A_x[a_x b_x] = \frac{\|b_x\|^2}{2a_x} + \frac{N_x}{2} \ln \frac{2\pi}{a_x}, \quad r_x[a_x b_x] = \frac{b_x}{a_x}, \quad v_x[a_x b_x] = \frac{1}{a_x}. \quad (37)$$

The log-partition, mean r_x^f and variance v_x^f for the factor marginal are equal to

$$A_f[a_f b_f] = \ln \int dx_f f(x_f) e^{-\frac{1}{2}a_f x_f^\top x_f + b_f^\top x_f}, \quad (38)$$

$$r_x^f[a_f b_f] = \partial_{b_{x \rightarrow f}} A_f[a_f b_f], \quad v_x^f[a_f b_f] = \langle \partial_{b_{x \rightarrow f}}^2 A_f[a_f b_f] \rangle, \quad (39)$$

where $\langle \rangle$ denotes the average over components. The moment-matching is equivalent to match the mean $r_x = r_x^f$ and variance $v_x = v_x^f$. In particular the $f \rightarrow x$ update in Algorithm 1 has to be understood as:

$$a_x^f = \frac{1}{v_x^f[a_f b_f]}, \quad b_x^f = \frac{r_x^f[a_f b_f]}{v_x^f[a_f b_f]}, \quad a_{f \rightarrow x}^{\text{new}} = a_x^f - a_{x \rightarrow f}, \quad b_{f \rightarrow x}^{\text{new}} = b_x^f - b_{x \rightarrow f}, \quad (40)$$

and the $x \rightarrow f$ update as:

$$a_x = \sum_{g \in x} a_{g \rightarrow x}, \quad b_x = \sum_{g \in x} b_{g \rightarrow x}, \quad a_{x \rightarrow f}^{\text{new}} = a_x - a_{f \rightarrow x}, \quad b_{x \rightarrow f}^{\text{new}} = b_x - b_{f \rightarrow x}. \quad (41)$$

When the variable x has only two neighbor factors, say f and g , the $x \rightarrow f$ update is particularly simple. The variable just passes through the corresponding messages:

$$a_{x \rightarrow f}^{\text{new}} = a_{g \rightarrow x}, \quad b_{x \rightarrow f}^{\text{new}} = b_{g \rightarrow x}. \quad (42)$$

Analytical vs approximate modules Many factor modules implemented in the tramp package can be analytically derived, which means providing an explicit formula for the factor log-partition $A_f[a_f b_f]$, mean $r_f[a_f b_f]$ and variance $v_f[a_f b_f]$. The following analytical modules are derived in Appendix B:

- linear channels which include the rotation channel, the discrete Fourier transform and convolutional filters as special cases;
- separable priors such as the Gaussian, binary, Gauss-Bernoulli, and positive priors;
- separable likelihoods such as the Gaussian or a deterministic likelihood like observing the sign, absolute value, modulus or phase;

- separable channels such additive Gaussian noise or the piecewise linear activation channel.

For other modules, that we did not manage to obtain analytically, one resorts to an approximation or an algorithm to estimate the log-partition $A_f[a_fb_f]$ and the associated mean $r_f[a_fb_f]$ and variance $v_f[a_fb_f]$. One such example in the tramp package is the low rank factorisation module $z = uv^\top$, for which we use the AMP algorithm developed in [Lesieur et al., 2017] to estimate $A_f[a_fb_f]$, $r_f[a_fb_f]$ and $v_f[a_fb_f]$.

MAP modules The maximum a posteriori (MAP) modules are worth mentioning especially due to their connection to proximal methods in optimization [Parikh and Boyd, 2014]. For any factor $f(x_f) = e^{-E_f(x_f)}$, one can use the Laplace method to obtain the MAP approximation to the log-partition, mean and variance:

$$A_f[a_fb_f] = -\min_{x_f} E_f(x_f|a_fb_f), \quad (43)$$

$$r_f[a_fb_f] = x_f^* = \arg \min_{x_f} E_f(x_f|a_fb_f), \quad (44)$$

$$v_f[a_fb_f] = \langle E_f''(x_f^*|a_fb_f)^{-1} \rangle \quad (45)$$

for $E_f(x_f|a_fb_f) = E_f(x_f) + \frac{a_f}{2}x_f^\top x_f - b_f^\top x_f$ and where $E_f''(x_f|a_fb_f)$ denotes the Hessian. These quantities can be expressed as:

$$A_f[a_fb_f] = \frac{\|b_f\|^2}{2a_f} - \mathcal{M}_{\frac{1}{a_f}E_f}\left(\frac{b_f}{a_f}\right), \quad (46)$$

$$r_f[a_fb_f] = \text{prox}_{\frac{1}{a_f}E_f}\left(\frac{b_f}{a_f}\right), \quad (47)$$

$$v_f[a_fb_f] = \langle \partial_{b_f} r_f[a_fb_f] \rangle \quad (48)$$

where we introduce the Moreau envelop $\mathcal{M}_g(y) = \min_x \{g(x) + \frac{1}{2}\|x - y\|^2\}$ and the proximal operator $\text{prox}_g(y) = \arg \min_x \{g(x) + \frac{1}{2}\|x - y\|^2\}$. Two such MAP modules are implemented in the tramp package for the penalties $E_f(x) = \lambda\|x\|_1$ and $E_f(x) = \lambda\|x\|_{2,1}$. The corresponding proximal operators are the soft thresholding and group soft thresholding operators.

2.7 Related algorithms

We recover several algorithms as special cases of Algorithm 1. For instance the G-VAMP [Schniter et al., 2017], TV-VAMP [Manoel et al., 2018] and ML-VAMP [Fletcher et al., 2018] algorithms correspond respectively to the factor graphs Figure 1 (a), (b) and (d). In this subsection, we explicit the equivalence with these algorithms and argue that the modularity of tramp allows to tackle a greater variety of inference tasks and optimization problems.

Inference in multi-layer network The ML-VAMP algorithm [Fletcher et al., 2018] performs inference in multi-layer networks such as Figure 1 (d). The one layer case reduces to the G-VAMP algorithm [Schniter et al., 2017] for GLM such as Figure 1 (a). Following Fletcher et al. [2018] let us consider the multi-layer model:

$$p(\mathbf{z}) = \prod_{l=0}^L p_l(z_l|z_{l-1}) \quad (49)$$

where $\mathbf{z} = \{z_l\}_{l=0}^L$ includes the measurement $y = z_L$ and the signals $\mathbf{x} = \{z_l\}_{l=0}^{L-1}$ to infer. The corresponding factor graph is displayed in Figure 3 (a). The model generally consists of a succession of linear channels (with possibly a bias and additive Gaussian noise) and separable non-linear activations; however, it is not necessary to specify further the architecture as all factors are treated on the same footing in both ML-VAMP and Algorithm 1.

We are interested in the isotropic Gaussian beliefs version of Algorithm 1. According to Eq. (42), the $z_l \rightarrow p_{l+1}$ update during the forward pass leads to

$$a_l^+ \doteq a_{p_l \rightarrow z_l} = a_{z_l \rightarrow p_{l+1}}, \quad b_l^+ \doteq b_{p_l \rightarrow z_l} = b_{z_l \rightarrow p_{l+1}}, \quad (50)$$

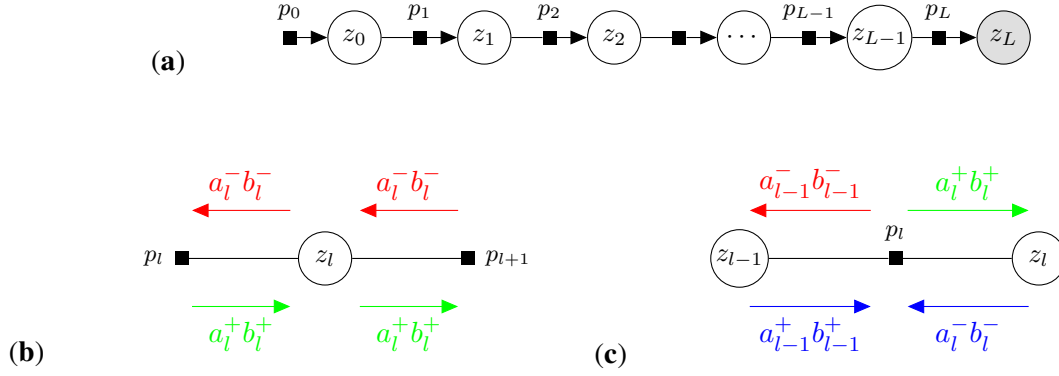


Figure 3: Message passing in ML-VAMP. **(a)** Multi-layer generalized linear model. **(b)** The variable z_l passes through the forward message $a_l^+ b_l^+$ (green) during the forward pass, and the backward message $a_l^- b_l^-$ (red) during the backward pass. **(c)** The factor p_l always takes as inputs the messages $a_{l-1}^+ b_{l-1}^+$ and $a_l^- b_l^-$ (blue). It outputs the message $a_l^+ b_l^+$ (green) during the forward pass, and the message $a_{l-1}^- b_{l-1}^-$ (red) during the backward pass.

while the $z_l \rightarrow p_l$ update during the backward pass leads to

$$a_l^- \doteq a_{p_{l+1} \rightarrow z_l} = a_{z_l \rightarrow p_l}, \quad b_l^- \doteq b_{p_{l+1} \rightarrow z_l} = b_{z_l \rightarrow p_l}. \quad (51)$$

Each variable in Figure 3 (a) has exactly two neighbors, so each variable just passes through the corresponding messages as illustrated in Figure 3 (b).

According to Eq. (40), the $p_l \rightarrow z_l$ update during the forward pass leads to

$$r_l = r_{z_l}^{p_l} [a_{l-1}^+ b_{l-1}^+ a_l^- b_l^-], \quad v_l = v_{z_l}^{p_l} [a_{l-1}^+ b_{l-1}^+ a_l^- b_l^-], \quad (52)$$

$$a_l = \frac{1}{v_l}, \quad b_l = \frac{r_l}{v_l}, \quad a_l^+ = a_l - a_l^-, \quad b_l^+ = b_l - b_l^-. \quad (53)$$

while the $p_l \rightarrow z_{l-1}$ update during the backward pass leads to

$$r_{l-1} = r_{z_{l-1}}^{p_l} [a_{l-1}^+ b_{l-1}^+ a_l^- b_l^-], \quad v_{l-1} = v_{z_{l-1}}^{p_l} [a_{l-1}^+ b_{l-1}^+ a_l^- b_l^-], \quad (54)$$

$$a_{l-1} = \frac{1}{v_{l-1}}, \quad b_{l-1} = \frac{r_{l-1}}{v_{l-1}}, \quad a_{l-1}^- = a_{l-1} - a_{l-1}^+, \quad b_{l-1}^- = b_{l-1} - b_{l-1}^+. \quad (55)$$

as illustrated in Figure 3 (c). The ML-VAMP algorithm parameterizes the messages using the precisions $\gamma_l^\pm = a_l^\pm$ and the means $r_l^\pm = b_l^\pm / a_l^\pm$ instead of the natural parameters a_l^\pm and b_l^\pm , but otherwise it is strictly equivalent to the EP Algorithm 1. Indeed the ML-VAMP algorithm computes during the forward pass:

$$\hat{z}_l^+ = r_l, \quad \eta_l^+ = a_l, \quad (56)$$

and updates the message according to:

$$\gamma_l^+ = \eta_l^+ - \gamma_l^-, \quad r_l^+ = (\eta_l^+ \hat{z}_l^+ - \gamma_l^- r_l^-) / \gamma_l^+ \quad (57)$$

which is identical to Eq. (53). Similarly the backward pass in the ML-VAMP algorithm is equivalent to Eq. (55). Finally the equivalence also holds for the prior $p_0(z_0)$ and the likelihood $p_L(y|z_{L-1})$. The prior is only used during the forward pass, it receives the backward message $a_0^- b_0^-$ as input and outputs the forward message $a_0^+ b_0^+$. The likelihood is only used during the backward pass, it receives the forward message $a_{L-1}^+ b_{L-1}^+$ as input and outputs the backward message $a_{L-1}^- b_{L-1}^-$.

Therefore the EP Algorithm 1 with isotropic Gaussian beliefs is exactly equivalent to the ML-VAMP algorithm. It offers a direct generalization to any tree-structured model, for instance the tree network of GLMs considered in [Reeves, 2017].

Optimization with non-separable penalties We now turn to the TV-VAMP algorithm [Manoel et al., 2018] designed to solve optimization problem of the form:

$$x^* = \arg \min \frac{1}{2\Delta} \|y - Ax\|^2 + \lambda f(Kx). \quad (58)$$

This corresponds to the MAP estimate for the factor graph displayed in Figure 4. Of particular interest is the case $K = \nabla$ and $f(z) = \|z\|_{2,1}$ which is identical to the total variation penalty for x .

We are interested in the version of Algorithm 1 with isotropic Gaussian beliefs on all variables except x for which we consider a full covariance belief. The penalty term λf would correspond to a factor $e^{-\lambda f(z)}$ in a probabilistic setting, but here we are only considering the MAP module for which the mean and variance are given by Eqs (47) and (48):

$$r_f[a_f b_f] = \eta_{\frac{\lambda}{a_f}} \left(\frac{b_f}{a_f} \right), \quad v_f[a_f b_f] = \frac{1}{a_f} \left\langle \nabla \eta_{\frac{\lambda}{a_f}} \left(\frac{b_f}{a_f} \right) \right\rangle, \quad (59)$$

where we introduce the function $\eta_\lambda(x) = \text{prox}_{\lambda f}(x)$ following Manoel et al. [2018].

First note that each variable in Figure 4 has exactly two neighbors. According to Eq. (42) the message passing is then particularly simple: the variable just passes through the corresponding messages. The Gaussian likelihood Δ (Appendix B.4.3) leads to the messages:

$$a_{a \rightarrow A} = a_{\Delta \rightarrow a} = \frac{1}{\Delta}, \quad b_{a \rightarrow A} = b_{\Delta \rightarrow a} = \frac{y}{\Delta}, \quad (60)$$

and the linear channel A with full covariance belief on x (Appendix B.2.11) leads to the messages:

$$a_{x \rightarrow K} = a_{A \rightarrow x} = \frac{A^\top A}{\Delta}, \quad b_{x \rightarrow K} = b_{A \rightarrow x} = \frac{A^\top y}{\Delta}. \quad (61)$$

This stream of constant messages from the likelihood Δ up to factor K is displayed on Figure 4. According to Eq. (40), the $K \rightarrow z$ update for the linear channel K with isotropic belief on z (Appendix B.2.1) leads to the messages:

$$r_x^K = \Sigma_x^K \left[\frac{A^\top y}{\Delta} + K^\top b_{z \rightarrow K} \right], \quad \Sigma_x^K = \left[\frac{A^\top A}{\Delta} + a_{z \rightarrow K} K^\top K \right]^{-1}, \quad (62)$$

$$r_z^K = K r_x^K, \quad v_z^K = \frac{1}{N_z} \text{Tr} [K \Sigma_x^K K^\top], \quad (63)$$

$$a_{z \rightarrow f} = a_{K \rightarrow z} = \frac{1}{v_z^K} - a_{z \rightarrow K}, \quad b_{z \rightarrow f} = b_{K \rightarrow z} = \frac{r_z^K}{v_z^K} - b_{z \rightarrow K}, \quad (64)$$

and the $f \rightarrow z$ update for the MAP module λf leads to the messages:

$$r_z^f = \eta_{\frac{\lambda}{a_{z \rightarrow f}}} \left(\frac{b_{z \rightarrow f}}{a_{z \rightarrow f}} \right), \quad v_z^f = \frac{1}{a_{z \rightarrow f}} \left\langle \nabla \eta_{\frac{\lambda}{a_{z \rightarrow f}}} \left(\frac{b_{z \rightarrow f}}{a_{z \rightarrow f}} \right) \right\rangle, \quad (65)$$

$$a_{z \rightarrow K} = a_{f \rightarrow z} = \frac{1}{v_z^f} - a_{z \rightarrow f}, \quad b_{z \rightarrow K} = b_{f \rightarrow z} = \frac{r_z^f}{v_z^f} - b_{z \rightarrow f}. \quad (66)$$

In [Manoel et al., 2018] the following quantities at iteration t are denoted by:

$$a_{z \rightarrow K} = \rho^t, \quad b_{z \rightarrow K} = u^t, \quad r_x^K = x^t, \quad v_z^K = \sigma_x^t, \quad r_z^f = z^t, \quad v_z^f = \sigma_z^t \quad (67)$$

Then Eqs (62), (65) and (66) are exactly equivalent to the Eqs (24), (25) and (26) of [Manoel et al., 2018] defining the TV-VAMP algorithm.

As discussed in greater detail by Manoel et al. [2018], the TV-VAMP algorithm is closely related to proximal methods: it can be viewed as the Peaceman-Rachford splitting where the step-size ρ^t is set adaptively. Then Algorithm 1 offers a generalization to any optimization problem for which the factor graph of penalty/constraints is tree-structured. For instance, while the TV-VAMP can only solve linear regression with a TV penalty, Algorithm 1 can be easily applied to a classification setting: one just needs to replace the Gaussian likelihood Δ by the appropriate likelihood. Also Algorithm 1 offers more flexibility in designing the approximate inference scheme: for example one can choose isotropic or diagonal Gaussian belief for x to alleviate the computational burden of inverting a matrix in Eq. (62).

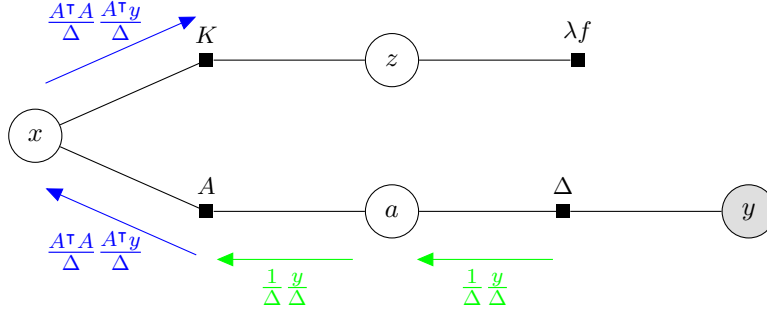


Figure 4: Message passing in TV-VAMP.

2.8 EP, EC, AdaTAP and Message-Passing

There is a long history behind the methods used in this section and the literature on statistical physics. In particular, broadening the class of matrices amenable to mean-field treatments was the motivation behind a decades long series of works.

Parisi and Potters [1995] were among the pioneers in this direction by deriving mean-field equations for orthogonal matrices. The adaTAP approach of Csató et al. [2002], and their reinterpretation as a particular case of the Expectation Propagation [Minka, 2001a] allowed for a generic reinterpretation of these ideas as an approximation of the log partition named Expectation Consistency (EC) [Heskes et al., 2005, Opper and Winther, 2005a,b]. Many works then applied these ideas to problems such as the perceptron [Shinzato and Kabashima, 2008b,a, Kabashima, 2003].

All these ideas were behind the recent renewal of interest of message-passing algorithms with generic rotationally invariant matrices [Schniter et al., 2017, Ma and Ping, 2017, Çakmak et al., 2014, 2016]. In a recent work, Maillard et al. [2019] showed the consistency and the equivalence of these approaches.

3 State evolution

In this Section, we show that (i) the state evolution can be formulated as the ensemble average of the EP updates, (ii) the free entropy potential is equal to the ensemble average EP approximation to the surprisal and (iii) we consistently find that the state evolution fixed point corresponds to a stationary point of the free entropy potential. To do so, we will first consider the high-dimensional limit of the variable and factor marginal and define the relevant ensemble average. Next, we will see that the state evolution can be reframed as several but equivalent optimization problems on potential functions, which all yield the measurements entropy as the global optimum. The duality between posterior overlaps/variances and precisions plays a crucial role and is a generalization of the I-MMSE relationship [Guo et al., 2005] and is similar to Reeves [2017] formalism.

3.1 Setting

While the EP algorithm can be applied to any probabilistic model and any choice of approximate beliefs, its performance in the high dimensional limit (the so-called state evolution formalism) is to date only derived for a restricted class of models. A very general setting is the tree network of GLMs proposed by Reeves [2017], which includes the GLM and multi-layer network as special cases, and applies to the EP algorithm with isotropic Gaussian beliefs. The state evolution is proven in the multi layer case [Fletcher et al., 2018] when the weight matrices in linear channels are drawn from an orthogonally invariant ensemble, but is expected to hold in the tree network case [Reeves, 2017]. In this section we shall not prove the state evolution formalism and refer the reader to the relevant publications. We will rather reformulate it as an equivalent but more interpretable ensemble average of the underlying EP algorithm, which furthermore can be modularized as done in the tramp package.

Teacher-student scenario Let us consider a tree-structured PGM $p(\mathbf{x}, \mathbf{y})$, for which the state evolution formalism holds, in the so-called teacher-student scenario. A teacher generates the true signals $\mathbf{x} = \{x\}$ and

measurements $\mathbf{y} = \{y\}$ from this model, and only communicates the measurements to the student, the student goal is to infer back the signals. While the state evolution holds in larger generality, tramp only implements the Bayes-optimal case where the student has full knowledge of the teacher generating distribution $p(\mathbf{x}, \mathbf{y})$ and assumes the exact same PGM to do the inference. To infer the signals, our student will use the EP Algorithm 1 with isotropic Gaussian beliefs which yields estimates of the posterior mean r_x and variance v_x for each signal x .

High dimensional limit In our PGM, each signal x and each measurement y is itself a high-dimensional vector or matrix (Figure 1). We are interested in the high dimensional regime where the dimension of each signal goes as $N_x = \alpha_x N$, where the scaling α_x are held fixed and $N \rightarrow \infty$. In that limit, we expect several EP quantities to self average, such as the variances v_x and v_f , the messages precisions $a_{x \rightarrow f}$ and $a_{f \rightarrow x}$, and the scaled log-partitions A_f and A_x . The state evolution equations derived in earlier publications actually give the time evolution of the ensemble average variances, from which the appropriate ensemble average can be read off. This ensemble average is defined at given message precisions (which may represent the typical precisions at iteration t of the EP algorithm) and is presented in Section 3.2.

EP performance The performance of the EP Algorithm 1 can be quantified by the mean squared error (MSE) obtained for each signal x , that is the MSE between the posterior mean r_x as estimated by EP and the ground truth value of x . In the Bayes-optimal setting this MSE is equal to v_x , the posterior variance as estimated by EP. Thus the state evolution also allows to track the performance of the EP algorithm at each iteration. The final MSE obtained (when the EP algorithm has converged) corresponds to a state evolution fixed point and can be shown to be a critical point of the replica free entropy potential [Manoel et al., 2017], or equivalently the Reeves [2017] potential. These two potentials will be shown to be equivalent and will be expressed in term of the ensemble average log-partitions A_f and A_x in Section 3.6.

Bayes-optimal vs hard phase The minimal MSE (MMSE) estimate of x and the MMSE itself are equal to the exact posterior mean and variance, given by the exact posterior marginal $p(x|\mathbf{y})$. The behaviour of AMP algorithms, such as EP Algorithm 1, has been investigated for a number of probabilistic models [Zdeborová and Krzakala, 2016]. For a large range of parameters specifying the model, AMP/EP is found to be Bayes-optimal and achieves the MMSE. However, for some regions of parameters known as the *hard phase* it fails to achieve the MMSE; but to date no polynomial time algorithm is known to achieve any better. Both the MSE achieved by EP and the MMSE are critical points of the free entropy potential, the MMSE corresponding though to the global minimizer.

3.2 Ensemble average at fixed precisions

Variable Let N_x be the dimension of the variable x . The ensemble average variance and scaled log-partition are given by:

$$v_x[a_x] = \mathbb{E} v_x[a_x b_x] = \frac{1}{a_x}, \quad (68)$$

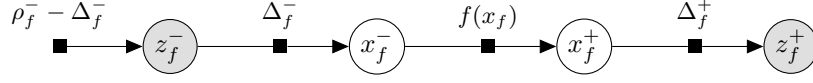
$$A_x[a_x] = \mathbb{E} \frac{1}{N_x} A_x[a_x b_x] = \frac{1}{2} a_x \rho_x - \frac{1}{2} + \frac{1}{2} \ln \frac{2\pi}{a_x}, \quad (69)$$

where $\rho_x = \mathbb{E} \frac{\|x\|_2^2}{N_x}$ is the second moment of x . The overlap between the signal x and the estimate r_x is equal to:

$$m_x[a_x] = \mathbb{E} \frac{r_x[a_x b_x] \cdot x}{N_x} = \rho_x - v_x[a_x]. \quad (70)$$

Eq. (68) is trivial because the instance variance $v_x[a_x b_x] = \frac{1}{a_x}$ is already independent of b_x . For the ensemble average log-partition, we have $A_x[a_x] = \frac{1}{2} a_x q_x + \frac{1}{2} \ln \frac{2\pi}{a_x}$ where $q_x = \mathbb{E} \frac{\|r_x\|_2^2}{N_x}$ is the self-overlap. But in the Bayes optimal setting $q_x = m_x = \rho_x - v_x$ which implies Eqs (69) and (70).

Factor Let's x_f^+ (resp. x_f^-) denote the set of output (resp. input) variables of the factor $f(x_f) = p(x_f^+ | x_f^-)$. We use this compact notation to deal with all cases (prior, channel, factorization, likelihood) having none to several inputs or outputs. Consider the elementary inference problem:



The teacher generates the signal x_f and measurements z_f from the probabilistic model:

$$p(x_f z_f | \Delta_f) = \mathcal{N}(z_f^+ | x_f^+ \Delta_f^+) f(x_f) \mathcal{N}(x_f^- | z_f^- \Delta_f^-) \mathcal{N}(z_f^- | 0, \rho_f^- - \Delta_f^-). \quad (71)$$

The student must infer the signals x_f from the noisy observations z_f . The posterior is equal to

$$p(x_f | a_f b_f) = f(x_f) e^{-\frac{1}{2} a_f x_f^T x_f + b_f^T x_f - A_f[a_f b_f]} \quad (72)$$

where $a_f = \frac{1}{\Delta_f}$ are the noise precisions and $b_f = \frac{z_f}{\Delta_f}$. We see that the student posterior corresponds to the factor marginal Eq. (14). In particular the log-partition of this elementary inference problem is $A_f[a_f b_f]$, the student estimate of the signals x_f is the posterior mean $r_f[a_f b_f]$ and the expected error is the posterior variance $v_f[a_f b_f]$. Let N_f be the dimension chosen to scale the factor f . The ensemble average variance and scaled log-partition are given by:

$$v_x^f[a_f] = \mathbb{E} v_x^f[a_f b_f], \quad (73)$$

$$A_f[a_f] = \mathbb{E} \frac{1}{N_f} A_f[a_f b_f], \quad (74)$$

and the overlap between the student estimate r_f and the ground truth x_f is equal to:

$$m_x^f[a_f] = \mathbb{E} \frac{r_x^f[a_f b_f] \cdot x}{N_x} = \rho_x - v_x^f[a_f], \quad (75)$$

where the expectation is over the teacher generative distribution Eq. (71).

3.3 Tramp implementation of state evolution

In the high dimensional limit we expect the variances and scaled log-partition to concentrate around their ensemble averages. Then the evolution of the variances in the tramp version of EP is simple to predict: we just have to replace the instance variance by the corresponding ensemble average, which yields the tramp implementation of state evolution summarized in Algorithm 2.

Algorithm 2: State evolution in tramp

output: precisions $\{a_x\}$

initialize $a_{x \rightarrow f}, a_{f \rightarrow x} = 0$

repeat

foreach edge $e \in E_+ \cup E_-$ **do**

 // forward and backward pass

if $e = f \rightarrow x$ **then**

$a_x^f = 1/v_x^f[a_f]$

 // variance-matching

$a_{f \rightarrow x}^{\text{new}} = a_x^f - a_{x \rightarrow f}$

 // message $f \rightarrow x$

if $e = x \rightarrow f$ **then**

$a_x = \sum_{g \in x} a_{g \rightarrow x}$

 // posterior

$a_{x \rightarrow f}^{\text{new}} = a_x - a_{f \rightarrow x}$

 // message $x \rightarrow f$

until convergence

The state evolution in [Fletcher et al., 2018], proved for the multi-layer network with orthogonally invariant weight matrices, exactly corresponds to Algorithm 2 applied to the chain graph Figure 1 (d).

3.4 Expression in term of mutual information

Variable During the inference procedure, we start from maximal uncertainty $H[\rho_x]$ about x to remaining uncertainty $H[v_x]$ after estimating x (estimate r_x and variance v_x). The information gain is therefore

$$I_x[a_x] = H[\rho_x] - H[v_x] = \frac{1}{N_x} I[x; r_x] = \frac{1}{2} \ln a_x \rho_x, \quad (76)$$

where $H[v] = \frac{1}{2} \ln 2\pi e v$ is the entropy a Gaussian variable with variance v . This is also the mutual information between the estimate r_x and the variable x . The mutual information $I_x[a_x]$ and average log-partition $A_x[a_x]$ are related by:

$$I_x[a_x] = \frac{1}{2} a_x \rho_x - A_x[a_x] + \frac{1}{2} \ln \frac{2\pi \rho_x}{e}. \quad (77)$$

Factor The mutual information between the measurements $z_f = \frac{b_f}{a_f}$ and the signals to infer x_f is equal to:

$$I_f[a_f] = \frac{1}{N_f} I[x_f; z_f] = \frac{1}{2} \sum_{x \in f} \alpha_x^f a_{x \rightarrow f} \rho_x - A_f[a_f] + \frac{1}{2} \sum_{x \in f_-} \alpha_x^f \ln \frac{2\pi \rho_x}{e}, \quad (78)$$

where $\alpha_x^f = \frac{N_x}{N_f}$ denotes the scaling² of the variable $x \in f$. If the factor has no inputs $f_- = \emptyset$ (for instance a prior) then the third term disappears.

3.5 Duality between overlaps/variances and precisions

Overlaps precisions duality The ensemble average $A_x[a_x]$ and $A_f[a_f]$ are convex functions. They provide the bijective mapping between the overlaps and precisions:

$$\frac{1}{2} m_x = \partial_{a_x} A_x[a_x], \quad \frac{1}{2} \alpha_x^f m_x^f = \partial_{a_{x \rightarrow f}} A_f[a_f], \quad (79)$$

$$\frac{1}{2} a_x = \partial_{m_x} A_x^*[m_x], \quad \frac{1}{2} \alpha_x^f a_{x \rightarrow f} = \partial_{m_x^f} A_f^*[m_f], \quad (80)$$

where we introduce the Legendre transformations of $A_x[a_x]$ and $A_f[a_f]$:

$$A_x^*[m_x] = \max_{a_x} \frac{1}{2} a_x m_x - A_x[a_x] = -\frac{1}{2} \ln 2\pi(\rho_x - m_x), \quad (81)$$

$$A_f^*[m_f] = \max_{a_f} \sum_{x \in f} \frac{1}{2} \alpha_x^f a_{x \rightarrow f} m_x^f - A_f[a_f]. \quad (82)$$

The relationship $\frac{1}{2} \alpha_x^f m_x^f = \partial_{a_{x \rightarrow f}} A_f$ is quite remarkable as it works for any kind of factors (prior, likelihood, linear, channel, factorization) and for all the variables attached to the factors (inputs and outputs). See Appendix C for a proof.

Variances precisions duality As $A_x[a_x]$ and $A_f[a_f]$ are convex, the mutual informations $I_x[a_x]$ and $I_f[a_f]$ are concave. They provide the bijective mapping between the variances and precisions:

$$\frac{1}{2} v_x = \partial_{a_x} I_x[a_x], \quad \frac{1}{2} \alpha_x^f v_x^f = \partial_{a_{x \rightarrow f}} I_f[a_f], \quad (83)$$

$$\frac{1}{2} a_x = -\partial_{v_x} I_x^*[v_x], \quad \frac{1}{2} \alpha_x^f a_{x \rightarrow f} = -\partial_{v_x^f} I_f^*[v_f], \quad (84)$$

where we introduce the Legendre transformations of $I_x[a_x]$ and $I_f[a_f]$:

$$I_x^*[v_x] = \max_{a_x} I_x[a_x] - \frac{1}{2} a_x v_x = \frac{1}{2} \ln \frac{\rho_x}{v_x} - \frac{1}{2}, \quad (85)$$

$$I_f^*[v_f] = \max_{a_x} I_f[a_f] - \sum_{x \in f} \frac{1}{2} \alpha_x^f a_{x \rightarrow f} v_x^f. \quad (86)$$

When the factor f is a prior, the relationship $\frac{1}{2} v_x^f = \partial_{a_{x \rightarrow f}} I_f$ is known as the I-MMSE relationship [Guo et al., 2005]. The duality between variances and precisions is almost identical to Reeves [2017] formalism, except that in tramp we define all quantities separately for the factor and variable marginals.

²For a separable factor, all the variables $x \in f$ will have the same dimension $N_x = N_f$ and $\alpha_x^f = 1$. For a factor that changes the variables dimensions, for instance the linear channel $x = Wz$, we will generally choose to scale the factor by the input dimension. In the linear channel case $N_f = N_z$ and $\alpha_z^f = 1$ and $\alpha_x^f = \frac{N_x}{N_z}$ which is the aspect ratio of the matrix W .

3.6 Graph decomposition of the free entropy

Let N be a dimension chosen to scale the entire model. The ensemble average of the surprisal is the measurements $\mathbf{y} = \{y\}$ entropy:

$$h = \frac{1}{N} \mathbb{E} F(\mathbf{y}) = -\frac{1}{N} \mathbb{E} \ln p(\mathbf{y}) = \frac{1}{N} H[\mathbf{y}]. \quad (87)$$

Let's introduce the precisions, overlaps and variances free entropy potentials:

$$A[\{a_x, a_f\}] = \sum_f \alpha_f A_f[a_f] + \sum_x \alpha_x (1 - n_x) A_x[a_x], \quad (88)$$

$$A^*[\{m_x\}] = \sum_f \alpha_f A_f^*[m_f] + \sum_x \alpha_x (1 - n_x) A_x^*[m_x], \quad (89)$$

$$I^*[\{v_x\}] = \sum_f \alpha_f I_f^*[v_f] + \sum_x \alpha_x (1 - n_x) I_x^*[v_x], \quad (90)$$

where we denote $\alpha_x = \frac{N_x}{N}$ the scaling of the variable x and $\alpha_f = \frac{N_f}{N}$ the scaling of the factor f . Actually due to Eqs (77) and (78), the overlaps and variances potentials are equal $A^*[m] = I^*[v]$. Alternatively, using the parametrization in term of variable to factor precisions $a_{x \rightarrow f}$ and factor to variable precisions $a_{f \rightarrow x}$:

$$A[\{a_{x \rightarrow f}, a_{f \rightarrow x}\}] = \sum_f \alpha_f A_f[a_f] - \sum_{x \in f} \alpha_x A_x[a_x^f] + \sum_x \alpha_x A_x[a_x] \quad (91)$$

$$a_f = \bigcup_{x \in f} a_{x \rightarrow f}, \quad a_x^f = a_{x \rightarrow f} + a_{f \rightarrow x}, \quad a_x = \sum_{f \in x} a_{f \rightarrow x}. \quad (92)$$

The parametrization Eq. (92) in term of messages has a nice interpretation: the variable precision is the sum of the incoming precisions (coming from the neighboring factors), the factor precision is the union of the incoming precisions (coming from the neighboring variables). The free entropy potentials can actually be seen as the ensemble average Minka and tramp free energy:

$$A[\{a_x, a_f\}] = \mathbb{E} \frac{1}{N} A[\{a_x, b_x, a_f, b_f\}], \quad (93)$$

$$A[\{a_{x \rightarrow f}, a_{f \rightarrow x}\}] = \mathbb{E} \frac{1}{N} A[\{a_{f \rightarrow x}, b_{f \rightarrow x}, a_{x \rightarrow f}, b_{x \rightarrow f}\}]. \quad (94)$$

Their graph decompositions Eqs (88) and (91) follow directly from the similar graph decomposition Eqs (28) and (29) of the Minka and tramp free energies.

Proposition 3 *The measurement entropy is obtained as:*

$$h = \min_{\{m_x\}} A^*[\{m_x\}] = \min_{\{v_x\}} I^*[\{v_x\}] \quad (95)$$

$$= \min_{\{a_x\}} \max_{\{a_f\}} -A[\{a_x, a_f\}] \quad s.t. \quad (n_x - 1)a_x = \sum_{f \in x} a_{x \rightarrow f} \quad (96)$$

$$= \min_{\{a_{f \rightarrow x}, a_{x \rightarrow f}\}} \text{extr} -A[\{a_{f \rightarrow x}, a_{x \rightarrow f}\}] \quad (97)$$

Besides, any stationary point of the potential functions (not necessarily the global optima) correspond to a state evolution fixed point:

$$v_x = v_x^f, \quad (n_x - 1)a_x = \sum_{f \in x} a_{x \rightarrow f}. \quad (98)$$

In Appendix D, we show that all these formulations are equivalent and all lead to a state evolution fixed point. The global minimizer of the free entropy potential gives the minimal mean square errors (MMSE) that are information-theoretically achievable. The mean square errors actually achieved by the EP Algorithm 1 are also a state evolution fixed point, or equivalently a stationary point of the potentials, which may or may not be the global optima depending on the task under consideration.

Remark 4 We recover the [Reeves \[2017\]](#) formalism ($I^*[v]$) proposed for tree GLM and the replica free entropy formula ($A^*[m]$) derived in [\[Gabri  et al., 2018\]](#) for multi-layer networks with orthogonally invariant weight matrices. Although it remains conjectural that the global minima of the free entropy potential yields the exact measurement entropy, it was rigorously proven by [Barbier et al. \[2019\]](#) for generalized linear models.

3.7 State evolution modules

For each factor module with isotropic Gaussian beliefs one can easily implement the corresponding state evolution module by taking the ensemble average presented in Section 3.2. For some modules there are closed-form expressions for the ensemble average log-partition $A_f[a_f]$ and variance $v_f[a_f]$: the linear channel (App. B.2.2), the Gaussian prior (App. B.3.4), the Gaussian likelihood (App. B.4.3) and the additive Gaussian noise channel (App. B.5.3). For separable factors $A_f[a_f]$ and $v_f[a_f]$ can be analytically obtained through a low dimensional integration: a one-dimensional integral for a separable prior (App. B.3.2), a two-dimensional integral for a separable likelihood (App. B.4.2) and a two-dimensional integral for a separable channel (App. B.5.2)

4 Examples

This section is dedicated to illustrating the tramp package. We first point out that its reconstruction performances asymptotically reaches the Bayes optimal limit out of the hard phase and that its fast execution speed often exceeds competing algorithms. Moreover we stress that the cornerstone of tramp is its modularity, which allows it to handle a wide range of inference tasks. To appreciate its great flexibility, we illustrate its performance on various tree-structured PGMs. Finally, the last section depicts the ability of tramp to predict its own state evolution performance on two simple GLMs: compressed sensing and sparse phase retrieval. All the codes corresponding to the examples presented in this section can be found at https://github.com/benjaminabuin/tramp_examples.

4.1 Benchmark on sparse linear regression

Let us consider a sparse signal $x \in \mathbb{R}^N$, iid drawn according to $x \sim \prod_{i=1}^N \mathcal{N}_\rho(x_i)$ where $\mathcal{N}_\rho = [1 - \rho]\delta + \rho\mathcal{N}$ is the Gauss-Bernoulli prior and \mathcal{N} the normal distribution. The inference task is to reconstruct the signal x from noisy observations $y \in \mathbb{R}^M$ generated according to

$$y = Ax + \xi \quad (99)$$

where $A \in \mathbb{R}^{M \times N}$ is the sensing matrix with iid Gaussian entries $A_{ji} \sim \mathcal{N}(0, 1/N)$ and ξ is a iid Gaussian noise $\xi \sim \mathcal{N}(0, \Delta)$. We define $\alpha = M/N$ the aspect ratio of the matrix A . The corresponding PGM is depicted in Figure 5.

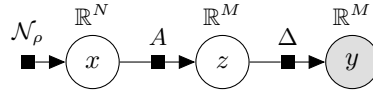


Figure 5: Sparse linear regression PGM.

The sparse linear regression problem can be easily solved with the tramp package. We simply need to import the necessary modules, declare the model, and run the Expectation Propagation algorithm:

```

1 # import modules
2 from tramp.base import Variable as V
3 from tramp.priors import GaussBernoulliPrior
4 from tramp.likelihoods import GaussianLikelihood
5 from tramp.channels import LinearChannel
6 # declare sparse linear regression model
7 model = (
8     GaussBernoulliPrior(rho=rho, size=N) @ V('x') @
9     LinearChannel(A) @ V('z') @
10    GaussianLikelihood(var=Delta, y=y)
11 ).to_model()
12 # run EP
13 from tramp.algos import ExpectationPropagation
14 ep = ExpectationPropagation(model)
15 ep.iterate(max_iter=200)

```

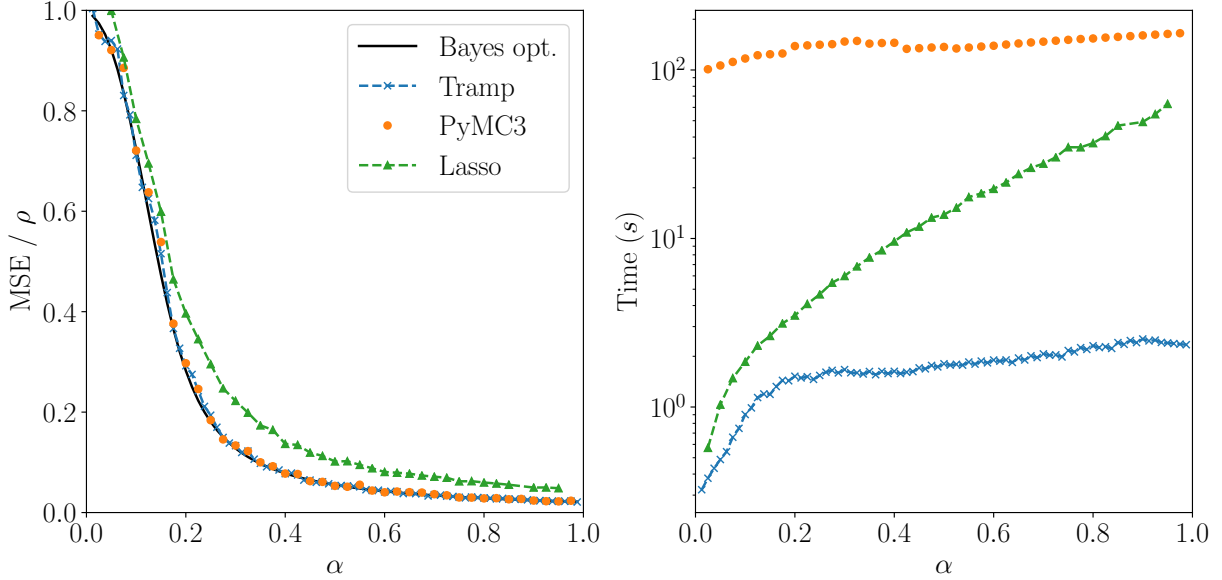


Figure 6: Benchmark on a sparse linear regression task: rescaled MSE as a function of $\alpha = M/N$. The MSE achieved by tramp (blue) is compared to the Bayes-optimal MMSE (black), Hamiltonian Monte-Carlo (orange) from PyMC3 (with $n_s = 1000$ distribution samples and NUTS sampler) and Lasso (green) from Scikit-Learn (with the regularization parameter set by cross-validation). The above experiments have been performed with parameters $(N, \rho, \Delta) = (1000, 0.05, 0.01)$ and have been averaged over 100 samples.

We compare the tramp performance on this inference task to the Bayes optimal theoretical prediction from Barbier et al. [2019] to two state of the art algorithms for this task: Hamiltonian Monte-Carlo from the PyMC3 package [Salvatier et al., 2016] and Lasso (L1-regularized linear regression) from the Scikit-Learn package [Pedregosa et al., 2011]. Note that to perform our experimental benchmark in Figure 6 the tramp and PyMC3 algorithms had access to the ground-truth parameters (ρ, Δ) used to generate the observations. In order to make the benchmark as fair as possible, we use the optimal regularization parameter for the Lasso, obtained by cross-validation.

We observe in Figure 6 (left) that for this model tramp is Bayes-optimal and reaches the MMSE, up to finite size fluctuations, just as PyMC3. They naturally both outperform Lasso from Scikit-Learn that never achieves the Bayes-optimal MMSE for the full range of aspect ratio α under investigation. This is expected and unfair to Lasso as the two Bayesian methods have full knowledge of the exact generating distribution in our toy model, but this is rarely the case in real applications.

Whereas the Hamiltonian Monte-Carlo algorithm requires to draw a large number of samples ($n_s = 10^3$) to reach a given threshold of precision, tramp is an iterative algorithm that converges in a few iterations varying broadly speaking between $[10^0; 10^2]$. It leads interestingly to an execution time smaller of two orders of magnitude with respect to PyMC3 as illustrated in Figure 6 (right). Hence the fast convergence and execution time of tramp is certainly a deep asset over PyMC3, or similar Markov Chain Monte-Carlo packages.

4.2 Depicting tramp modularity

In order to show the remarkable adaptability and modularity of tramp to handle various inference tasks, we present here different examples where the prior distributions are modified flexibly. In particular, we consider first Gaussian denoising of synthetic data with either sparse discrete Fourier transform (DFT) or sparse gradient, and second the denoising and inpainting of real images drawn from the MNIST data set, using a trained Variational Auto-Encoder (VAE) as a prior.

4.2.1 Sparse DFT/gradient denoising

Let us consider a signal $x \in \mathbb{R}^N$ corrupted by a Gaussian noise $\xi \sim \mathcal{N}(0, \Delta)$, that leads to the observation $y \in \mathbb{R}^N$ according to

$$y = x + \xi \quad (100)$$

In contrast to the first section in which we considered the signal x to be sparse, we assume here that the signal is dense but that a linear transformation of the signal is sparse. In other words let us define the variable $z = \Omega x$ that we assume to be sparse, where Ω denotes a linear operator acting on the signal. The PGM associated to this model is depicted in Figure 7.

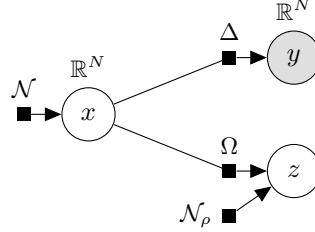


Figure 7: PGM for sparse Ω denoising, where Ω represents either the DFT or the gradient operator.

As a matter of clarity, we focus on two toy one-dimensional signals:

1. $x \in \mathbb{R}^N$ such that $\forall i \in [1 : N], x_i = \cos(t_i) + \sin(2t_i)$, with $t_i = 2\pi(-1 + \frac{2i}{N})$. The signal is sparse in the Fourier basis with only two spikes, that leads us to consider a sparse DFT prior: Ω is the discrete Fourier transform,
2. $x \in \mathbb{R}^N$ such that it is randomly drawn constant by pieces. Its gradient contains a lot of zeros and therefore inference with a sparse gradient prior is appropriate: Ω is the gradient operator.

After importing the relevant modules, declaring the model in the tramp package is simple, for instance for the sparse gradient model:

```
1 # sparse gradient denoising
2 model = (
3     GaussianPrior(size=N) @ V('x', n_prev=1, n_next=2) @ (
4         GaussianLikelihood(var=Delta, y=y) + (
5             GradientChannel() +
6             GaussBernoulliPrior(rho=rho, size=(1,N))
7         ) @ V('z', n_prev=2, n_next=0)
8     )
9 ).to_model()
```

For the sparse DFT model, one just needs to replace `GradientChannel` by `DFTChannel`. Numerical experiments are shown in Figure 8. The left panel shows the observation y , while the middle and right panels illustrate the tramp reconstruction of the signal \hat{x} and of its linear transform \hat{z} compared to the ground truth x^* and z^* . The tramp reconstruction approaches closely the ground truth signal and leads to $\text{MSE} \sim 10^{-2}/10^{-3}$ for signals $1/2$.

4.2.2 Variational Auto-Encoder on MNIST

Let us consider a signal $x \in \mathbb{R}^N$ (with $N = 784$) drawn from the MNIST data set. We want to reconstruct the original image from a corrupted observation $y = \varphi(x) \in \mathbb{R}^N$, where $\varphi : \mathbb{R}^N \rightarrow \mathbb{R}^N$ represents a noisy channel. In the following the noisy channel represents either a Gaussian additive channel or an inpainting channel, that erases some pixels of the input image.

In order to reconstruct correctly the MNIST image, we investigated the possibility of using a generative prior such as a Variational Auto-Encoder (VAE) along the lines of [Bora et al. \[2017\]](#), [Fletcher et al. \[2018\]](#). The information theoretical and approximate message passing properties of reconstruction of a low rank or

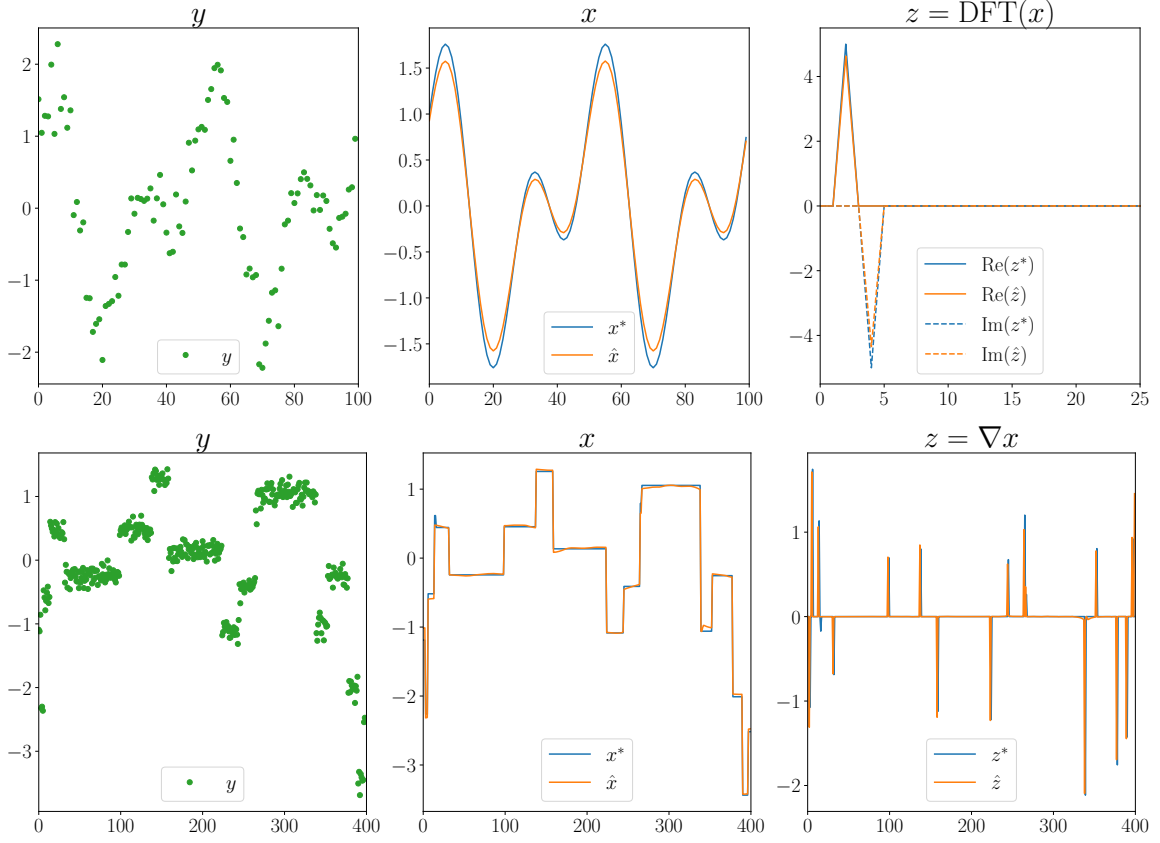


Figure 8: Sparse FFT/gradient denoising: **(left)** noisy observation y , **(middle)** ground truth signal x^* and predicted \hat{x} and **(right)** ground truth linear transform z^* and predicted \hat{z} for **(upper)** sparse DFT denoising with $(N, \rho, \Delta) = (100, 0.02, 0.1)$ and **(lower)** sparse gradient denoising with $(N, \rho, \Delta) = (400, 0.04, 0.01)$.

GLM channel, using a dense feed-forward neural network generative prior with iid weights has been studied in particular in [Aubin et al., 2019b,a]. The VAE architecture is summarized in Figure 9 and the training procedure on the MNIST data set follows closely the canonical one detailed in [Keras-VAE]. We considered two common inference tasks: denoising and inpainting.

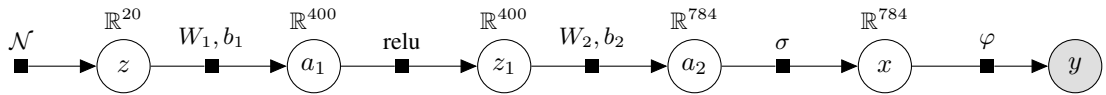


Figure 9: Denoising/inpainting a MNIST image with a VAE prior. The weights W_1, W_2 and biases b_1, b_2 were learned beforehand on the MNIST data set.

Denoising: In that case, the corrupted channel $\varphi_{\text{den}, \Delta}$ adds a Gaussian noise and corresponds to the noisy channel

$$\varphi_{\text{den}, \Delta}(x) = x + \xi \quad \text{with} \quad \xi \sim \mathcal{N}(0, \Delta).$$

Inpainting: The corrupted channel erases a few pixels of the input image and corresponds formally to

$$\varphi_{\text{inp}, I_\alpha}(x) = \begin{cases} 0 & \text{if } i \in I_\alpha, \\ x_i & \text{otherwise.} \end{cases}$$

where I_α denotes the set of erased indexes of size $\lfloor \alpha N \rfloor$ for some $\alpha \in [0, 1]$. As an illustration, we consider two different manners of generating the erased interval I_α :

1. A central horizontal band of width $\lfloor \alpha N \rfloor$: $I_\alpha^{\text{band}} = [\lfloor \frac{N}{2}(1 - \alpha) \rfloor; \lfloor \frac{N}{2}(1 + \alpha) \rfloor]$

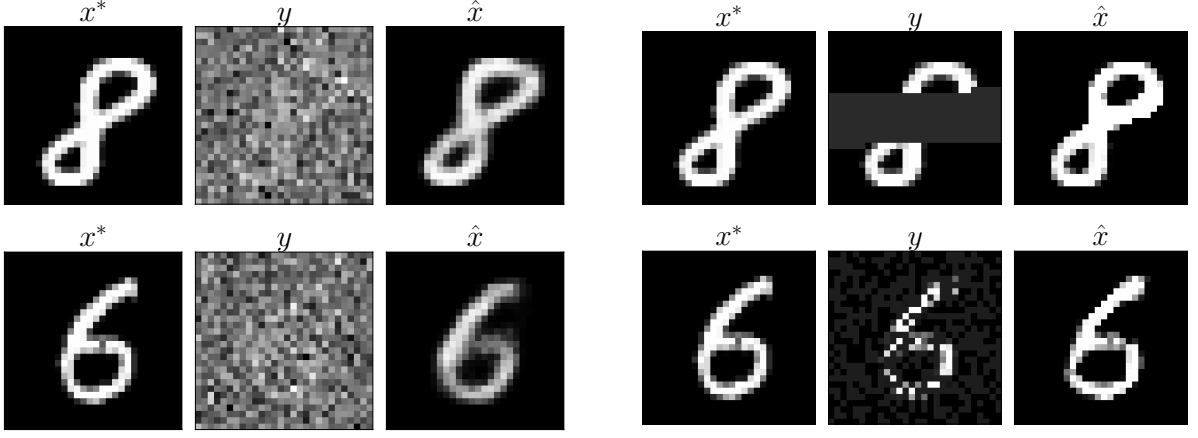


Figure 10: Illustration of the tramp prediction \hat{x} using a VAE prior from observation $y = \varphi(x^*)$ with x^* a MNIST sample. **(left)** Denoising $\varphi = \varphi_{\text{den}, \Delta}$ with $\Delta = 4$. **(right-upper)** Band-inpainting $\varphi_{\text{inp}, I_{\alpha}^{\text{band}}}$ with $\alpha = 0.3$ **(right-lower)** Uniform-inpainting $\varphi_{\text{inp}, I_{\alpha}^{\text{uni}}}$ with $\alpha = 0.5$.

2. Indices drawn uniformly at random $[\alpha N] : I_{\alpha}^{\text{uni}} \sim \text{U}([1, N]; [\alpha N])$

Solving these inference tasks in tramp is straightforward: first declare the model Figure 9 and then run Expectation Propagation as exemplified in Section 4.1 for the sparse regression case. A few MNIST samples x^* compared to the noisy observations y and tramp reconstructions \hat{x} are presented in Figure 10, that suggest that tramp is able to use the trained VAE prior information to either denoise very noisy observations or reconstruct missing pixels.

4.3 Theoretical prediction of performance

Previous sections were devoted to applications of the Expectation Propagation (EP) Algorithm 1 implemented in tramp. Moreover the state evolution (SE) Algorithm 2 has also been implemented in the package. This two-in-one package makes it easier and powerful to obtain performances of the EP algorithm on finite size instances as well as the infinite size limit behavior predicted by the state evolution.

We illustrate this on two generalized linear models: *compressed sensing* and *sparse phase retrieval*, whose common PGM is represented in Figure 11. Briefly, we consider a sparse $x \in \mathbb{R}^N$ iid drawn from a Gauss-Bernoulli distribution \mathcal{N}_{ρ} . We observe $y \in \mathbb{R}^M = \varphi(Ax)$ with $A \in \mathbb{R}^{M \times N}$ a Gaussian iid matrix, and the noiseless channel is $\varphi(x) = x$ in the compressed sensing case and $\varphi(x) = |x|$ in the phase retrieval one.

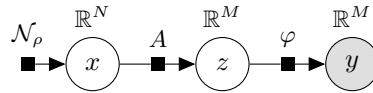


Figure 11: Graphical model representing the compressed sensing ($\varphi(x) = x$) and phase retrieval ($\varphi(x) = |x|$). We denote $\alpha = M/N$ the aspect ratio of the sensing matrix A .

Getting the MSE predicted by state evolution is straightforward in the tramp package. After importing the relevant modules, one just needs to declare the model and run the SE algorithm. For instance for the sparse phase retrieval model:

```

1 # declare sparse phase retrieval model
2 model = (
3     GaussBernoulliPrior(rho=rho, size=N) @ V('x') @
4     LinearChannel(A) @ V('z') @
5     AbsLikelihood(y=y)
6 ).to_model()
7 # run SE
8 from tramp.algos import StateEvolution
9 se = StateEvolution(model)
10 se.iterate(max_iter=200)

```

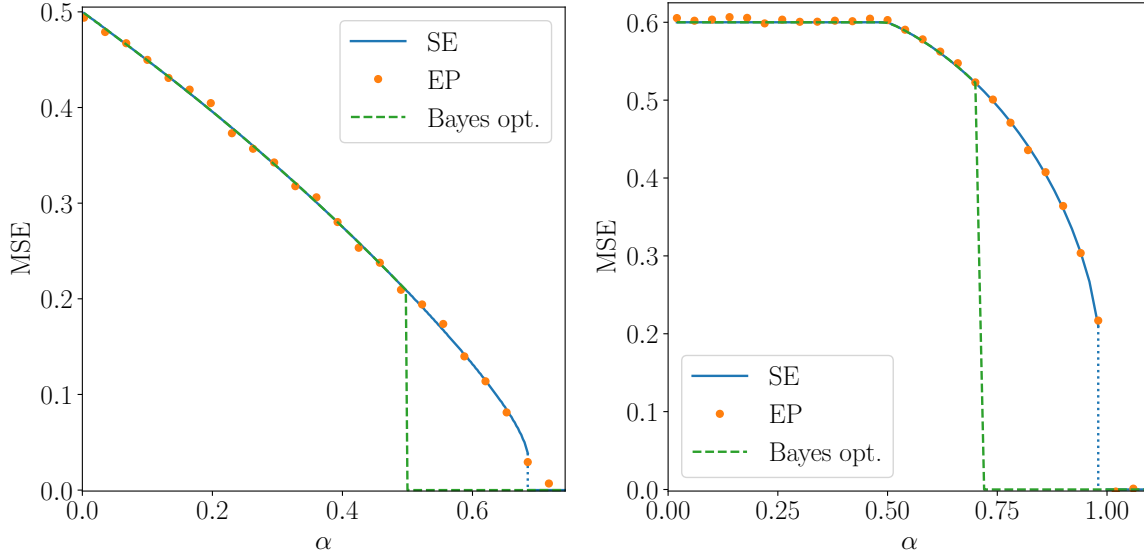


Figure 12: MSE as a function of $\alpha = M/N$ for **(left)** Compressed sensing ($\rho = 0.5$), **(right)** Sparse phase retrieval ($\rho = 0.6$).

In Figure 12, we compare the MSE theoretically predicted by state evolution and the MSE obtained on high-dimensional ($N = 2000$) instances of EP. Notably up to finite size effects, the MSE averaged over 25 instances of EP match perfectly the MSE predicted by SE. Also the MSE is equal to the Bayes optimal MMSE proven in [Barbier et al., 2019], except for a region of α values known as the hard phase. In that phase, there is a significant gap between the MMSE that is information-theoretically achievable and the MSE actually achieved by EP.

Note that the MMSE is also a state evolution fixed point (Proposition 3) and can thus be obtained by initializing the SE Algorithm 2 in the right basin of attraction. For the two models discussed here, we found that initializing the incoming prior message $a_{x \rightarrow \mathcal{N}_p} \gg 1$ was sufficient to converge towards the MMSE and obtain the Bayes optimal curve.

5 Discussion

Modularity The tramp package aims to solve compositional inference tasks, which can be broken down into local inference problems. As long as the underlying factor graph is tree-structured, the global inference task can be solved by message passing using Algorithm 1, which is just a particular instance of EP. Note that Algorithm 1 is generic, meaning that it can be implemented independently of the probabilistic graphical model under consideration. The main strength of the presented approach is therefore its modularity. In the tramp package, each module corresponds to a local inference problem given by a factor and associated beliefs on its variables. As long as the module is implemented (which means computing the log-partition $A_f[\lambda_f]$ and the moment function $\mu_f[\lambda_f]$), it can be composed at will with other modules to solve complex inference tasks. Several popular machine learning tasks can be reformulated that way as illustrated in Figure 1. We hope that the tramp package offers a unifying framework to run these models, as well as study them theoretically using the state evolution and free entropy formalism. Below, we review some shortcomings of the tramp package and possible ways to overcome them.

Hyper-parameter learning In principle, it should be straightforward to learn hyper-parameters. As usually done in hierarchical Bayesian modelling, one simply needs to add the hyper-parameters as scalar variables in the graphical model with associated hyper priors. In term of the tramp package, one would simply need to implement the corresponding module (where the set of variables of the factor now includes the hyper-parameters to learn). In the typical use case, where the signals are high dimensional but the hyper-parameters are just scalars, Algorithm 1 will likely be equivalent to the Expectation-Maximization [Dempster et al., 1977] learning of hyper-parameters, as usually done in AMP algorithms [Krzakala et al., 2012].

Generic belief While the message passing Algorithm 1 is formulated for any kind of beliefs, the current tramp implementation only supports isotropic Gaussian beliefs. However we could consider more generic beliefs to deal with more complicated types of variable, such as Gaussian process beliefs [Rasmussen and Williams, 2006] for functions or harmonic exponential family beliefs [Cohen and Welling, 2015] for elements of compact groups. Maybe one can recover algorithms similar to [Oppor and Winther, 2000] for Gaussian process classification or [Perry et al., 2018] for synchronisation problems over compact groups, and reformulate them in a more modular way. Even if we restrict ourselves to Gaussian beliefs, it may be beneficial to go beyond the isotropic case and consider diagonal or full covariance beliefs [Oppor and Winther, 2005a], or any kind of prescribed covariance structure. As exemplified in the committee machine keeping a covariance between experts leads to a more accurate algorithm [Aubin et al., 2018].

Beyond trees By design, the tramp package can only handle tree-structured factor graphs. To overcome this fundamental limitation and extend to generic factor graphs, one could use the Kikuchi free energy [Yedidia and Freeman, 2001] in place of the Bethe free energy as a starting point. Similar to the Bethe free energy which is exact for tree-structured factor graphs, the Kikuchi free energy will be exact if the graphical model admits a hyper-tree factorization [Wainwright and Jordan, 2008]. The minimization of the Kikuchi free energy under weak consistency constraints [Zoeter and Heskes, 2005] could be used to implement a generalization of Algorithm 1, however the message passing will be more challenging than in the tree case. An equivalent of Proposition 1 will likely hold, where the graph decomposition Eqs (27)-(28) found for the Gibbs and Minka free energies will be replaced by the hyper-tree factorization.

Convergence The message passing Algorithm 1, like other EP algorithms, is not guaranteed to converge. This is a major drawback, and indeed on some instances the naive application of Algorithm 1 will diverge. Double loop algorithms like [Heskes and Zoeter, 2002] will ensure convergence, but are unfortunately very slow. In practice, damping the updates is often sufficient to converge towards a fixed point. In the tramp package the amount of damping has to be chosen by the user. It will be therefore interesting to generalize the adaptive damping scheme [Vila et al., 2015] in order to tune this damping automatically.

Proofs In Section 3, we merely stated the state evolution and the free entropy formalism, but did not provide any rigorous proof. We instead relied upon earlier derivations of these results for specific models. For instance in the multi-layer model with orthogonally invariant weight matrices, the state evolution was rigorously proven by Fletcher et al. [2018] while the free potential was heuristically derived using the replica method [Gabri   et al., 2018]. When the weight matrices are Gaussian, the replica free entropy can further be shown to be rigorous [Reeves and Pfister, 2016, Barbier et al., 2019]. One extension of our work would be to generalize existing proofs to arbitrary tree factor graphs.

Acknowledgments

This work is supported by the ERC under the European Union’s Horizon 2020 Research and Innovation Program 714608-SMiLe, as well as by the French Agence Nationale de la Recherche under grant ANR-17-CE23-0023-01 PAIL. Additional funding is acknowledged by AB from ‘Chaire de recherche sur les mod  les et sciences des donn  es’, Fondation CFM pour la Recherche-ENS.

A Proof of Proposition 1

A.1 Minimization of $G[\{\mu_x\}]$

First let's minimize the Bethe free energy at fixed moments $\mu = \{\mu_x\}$:

$$F_\mu = \min_{\{q_f, q_x\} \in \mathcal{M}_\mu} F_{\text{Bethe}}[\{q_f, q_x\}] \quad (101)$$

where \mathcal{M}_μ is the set of factor and variable marginals at fixed moment:

$$\mathcal{M}_\mu = \{ \{q_x, q_f\} : \forall x, \forall f \in x, \mathbb{E}_{q_x} \phi(x) = \mathbb{E}_{q_f} \phi(x) = \mu_x \}. \quad (102)$$

The solution will be a stationary point of the Lagrangian

$$\begin{aligned} \mathcal{L}[\{q_f, q_x, \lambda_{x \rightarrow f}, \lambda_x\}] &= F_{\text{Bethe}}[\{q_f, q_x\}] \\ &+ \sum_f \sum_{x \in f} \lambda_{x \rightarrow f}^\top (\mu_x - \mathbb{E}_{q_f} \phi(x)) + \sum_x (1 - n_x) \lambda_x^\top (\mu_x - \mathbb{E}_{q_x} \phi(x)) \end{aligned} \quad (103)$$

with Lagrange multipliers $\lambda_{x \rightarrow f}$ and λ_x associated to the moment constraint $\mathbb{E}_{q_f} \phi(x) = \mu_x$ and $\mathbb{E}_{q_x} \phi(x) = \mu_x$. Then $0 = \delta_{q_x} \mathcal{L} = \delta_{q_f} \mathcal{L} = \partial_{\lambda_{x \rightarrow f}} \mathcal{L}$ leads to the solution:

$$q_f^*(x_f) = f(x_f) e^{\lambda_f^\top \phi(x_f) - A_f[\lambda_f]}, \quad (104)$$

$$q_x^*(x) = e^{\lambda_x^\top \phi(x) - A_x[\lambda_x]}, \quad (105)$$

$$\lambda_f = \{\lambda_{x \rightarrow f}\}_{x \in f}, \quad (106)$$

$$\mu_x = \mu_x[\lambda_x] = \mu_x^f[\lambda_f]. \quad (107)$$

Besides the minimal F_μ is equal to:

$$\begin{aligned} F_\mu &= \sum_f F_f[q_f^*] + \sum_x (1 - n_x) F_x[q_x^*] \\ &= \sum_f \text{KL}[q_f^* \| f] + \sum_x (1 - n_x) (-H[q_x^*]) \\ &= \sum_f G[\mu_f] + \sum_x (1 - n_x) G_x[\mu_x] \\ &= G[\mu]. \end{aligned}$$

But then:

$$F_\phi = \min_\mu \min_{\{q_f, q_x\} \in \mathcal{M}_\mu} F_{\text{Bethe}} = \min_\mu F_\mu = \min_\mu G[\mu]. \quad (108)$$

Besides, minimizing $G[\mu]$ leads to:

$$0 = \partial_{\mu_x} G[\mu] = \sum_{f \in x} \lambda_{x \rightarrow f} + (1 - n_x) \lambda_x \quad (109)$$

which is the natural parameter constraint. The solution is therefore the same as the EP fixed point Eq. (34).

A.2 Stationary point of $A[\{\lambda_x, \lambda_f\}]$

Using the duality between natural parameters and moments:

$$\begin{aligned}
\min_{\mu} G[\mu] &= \min_{\mu} \sum_f G_f[\mu_f] + \sum_x (1 - n_x) G_x[\mu_x] \\
&= \min_{\mu} \sum_f \max_{\lambda_f} \left\{ \lambda_f^\top \mu_f - A_f[\lambda_f] \right\} + \sum_x \underbrace{(1 - n_x)}_{\leq 0} \max_{\lambda_x} \left\{ \lambda_x^\top \mu_x - A_x[\lambda_x] \right\} \\
&= \min_{\mu} \min_{\lambda_x} \max_{\lambda_f} - \sum_f A_f[\lambda_f] - \sum_x (1 - n_x) A_x[\lambda_x] \\
&\quad + \sum_x \mu_x^\top \left[\sum_{f \in x} \lambda_{x \rightarrow f} + (1 - n_x) \lambda_x \right] \\
&= \min_{\lambda_x} \max_{\lambda_f} -A[\{\lambda_x, \lambda_f\}] \quad \text{s.t.} \quad (n_x - 1) \lambda_x = \sum_{f \in x} \lambda_{x \rightarrow f}. \tag{110}
\end{aligned}$$

As a consistency check, let's directly derive the solution to Eq. (110). Consider the Lagrangian

$$\mathcal{L}[\{\lambda_f, \lambda_x, \mu_x\}] = A[\{\lambda_x, \lambda_f\}] + \sum_x \mu_x^\top \left[(n_x - 1) \lambda_x - \sum_{f \in x} \lambda_{x \rightarrow f} \right] \tag{111}$$

with Lagrangian multiplier μ_x associated to the constraint $(n_x - 1) \lambda_x = \sum_{f \in x} \lambda_{x \rightarrow f}$. At a stationary point:

$$\partial_{\mu_x} \mathcal{L} = 0 \implies (n_x - 1) \lambda_x = \sum_{f \in x} \lambda_{x \rightarrow f} \tag{112}$$

$$\partial_{\lambda_f} \mathcal{L} = 0 \implies \mu_x = \mu_x^f[\lambda_f] \tag{113}$$

$$\partial_{\lambda_x} \mathcal{L} = 0 \implies \mu_x = \mu_x[\lambda_x] \tag{114}$$

which is exactly the same as the EP fixed point Eq. (34). Furthermore the Lagrangian multiplier is the posterior moment $\mu_x = \mu_x^*$.

A.3 Stationary point of $A[\{\lambda_{x \rightarrow f}, \lambda_{f \rightarrow x}\}]$

Finally, the optimization under constraint of $A[\{\lambda_x, \lambda_f\}]$ is equivalent to finding a stationary point of $A[\{\lambda_{f \rightarrow x}, \lambda_{x \rightarrow f}\}]$ without any constraint. Indeed:

$$\partial_{\lambda_{f \rightarrow x}} A = 0 \implies \mu_x[\lambda_x^f] = \mu_x[\lambda_x] \implies \lambda_x^f = \lambda_x \tag{115}$$

$$\partial_{\lambda_{x \rightarrow f}} A = 0 \implies \mu_x^f[\lambda_f] = \mu_x[\lambda_x^f] \tag{116}$$

which implies the natural parameter constraint

$$\sum_{f \in x} \lambda_{x \rightarrow f} = \sum_{f \in x} (\lambda_x^f - \lambda_{f \rightarrow x}) = n_x \lambda_x - \lambda_x = (n_x - 1) \lambda_x \tag{117}$$

and the moment matching $\mu_x^f[\lambda_f] = \mu_x[\lambda_x]$ defining the EP fixed point Eq. (34).

B Tramp modules

B.1 Variable

The tramp package only implements isotropic Gaussian beliefs, but the variable log-partitions presented here will be useful to derive the factor modules.

B.1.1 General variable

An approximate belief, which we may as well call a variable type, is specified by the base space X as well as the chosen set of sufficient statistics $\phi(x)$. Any variable type defines an exponential family distribution

$$p(x|\lambda) = e^{\lambda^\top \phi(x) - A[\lambda]} \quad (118)$$

indexed by the natural parameter λ . The family can be alternatively indexed by the moments $\mu = \mathbb{E}\phi(x)$. The log-partition

$$A[\lambda] = \ln \int_X dx e^{\lambda^\top \phi(x)} \quad (119)$$

provides the bijective mapping between the natural parameters and the moments:

$$\mu[\lambda] = \partial_\lambda A[\lambda]. \quad (120)$$

For all the variable types considered below, we will always have $x \in \phi(x)$ in the set of sufficient statistics. Its associated natural parameter $b \in \lambda$ is thus dual to the mean $r \in \mu$. The mean and variance are given by:

$$r[\lambda] = \partial_b A[\lambda], \quad v[\lambda] = \partial_b^2 A[\lambda], \quad (121)$$

We list below the log-partition, mean and variance for several variable types, which correspond to well known exponential family distributions.

B.1.2 Isotropic Gaussian variable

For $x \in \mathbb{R}^N$, sufficient statistics $\phi(x) = \{x, -\frac{1}{2}x^\top x\}$, natural parameters $b \in \mathbb{R}^N$ and scalar precision $a \in \mathbb{R}$.

$$A[ab] = \ln \int dx e^{-\frac{1}{2}ax^\top x + b^\top x} = \frac{\|b\|^2}{2a} + \frac{N}{2} \ln \frac{2\pi}{a}, \quad (122)$$

$$r[ab] = \frac{b}{a}, \quad v[ab] = \frac{1}{a} \in \mathbb{R}. \quad (123)$$

The corresponding exponential family is the isotropic multivariate Normal:

$$p(x|ab) = \mathcal{N}(x|rv) \quad \text{with} \quad r = \frac{b}{a}, \quad v = \frac{1}{a}. \quad (124)$$

B.1.3 Diagonal Gaussian variable

For $x \in \mathbb{R}^N$, sufficient statistics $\phi(x) = \{x, -\frac{1}{2}x^2\}$, natural parameters $b \in \mathbb{R}^N$ and diagonal precision $a \in \mathbb{R}^N$.

$$A[ab] = \ln \int dx e^{-\frac{1}{2}x^\top ax + b^\top x} = \sum_{i=1}^N \frac{b_i^2}{2a_i} + \frac{1}{2} \ln \frac{2\pi}{a_i}, \quad (125)$$

$$r[ab] = \frac{b}{a}, \quad v[ab] = \frac{1}{a} \in \mathbb{R}^N. \quad (126)$$

The corresponding exponential family is the diagonal multivariate Normal:

$$p(x|ab) = \mathcal{N}(x|rv) \quad \text{with} \quad r = \frac{b}{a}, \quad v = \frac{1}{a}. \quad (127)$$

B.1.4 Full covariance Gaussian variable

For $x \in \mathbb{R}^N$, sufficient statistics $\phi(x) = \{x, -\frac{1}{2}xx^\top\}$, natural parameters $b \in \mathbb{R}^N$ and matrix precision $a \in \mathbb{R}^{N \times N}$.

$$A[ab] = \ln \int dx e^{-\frac{1}{2}x^\top ax + b^\top x} = \frac{1}{2}b^\top a^{-1}b + \frac{1}{2} \ln \det 2\pi a^{-1}, \quad (128)$$

$$r[ab] = \frac{b}{a}, \quad \Sigma[ab] = a^{-1} \in \mathbb{R}^{N \times N}, \quad (129)$$

The corresponding exponential family is the full covariance multivariate Normal:

$$p(x|ab) = \mathcal{N}(x|r\Sigma) \quad \text{with} \quad r = \frac{b}{a}, \quad \Sigma = a^{-1}. \quad (130)$$

B.1.5 Real variable

For $x \in \mathbb{R}$, sufficient statistics $\phi(x) = \{x, -\frac{1}{2}x^2\}$, natural parameters $\{b, a\}$.

$$A[ab] = \ln \int dx e^{-\frac{1}{2}ax^2 + bx} = \frac{b^2}{2a} + \frac{1}{2} \ln \frac{2\pi}{a}, \quad (131)$$

$$r[ab] = \frac{b}{a}, \quad v[ab] = \frac{1}{a}. \quad (132)$$

The corresponding exponential family is the Normal:

$$p(x|ab) = \mathcal{N}(x|rv) \quad \text{with} \quad r = \frac{b}{a}, \quad v = \frac{1}{a}. \quad (133)$$

B.1.6 Binary variable

For $x \in \pm$, sufficient statistics $\phi(x) = \{x\}$, natural parameter $\{b\}$.

$$A[b] = \ln \sum_{x=\pm} e^{bx} = \ln(e^b + e^{-b}), \quad (134)$$

$$r[b] = \tanh(b), \quad v[b] = \frac{1}{\cosh(b)^2}. \quad (135)$$

The corresponding exponential family is the Bernoulli (over \pm):

$$p(x|b) = p_+ \delta_{+1}(x) + p_- \delta_{-1}(x) \quad (136)$$

where the natural parameter $b = \frac{1}{2} \ln \frac{p_+}{p_-}$ is the log-odds.

B.1.7 Sparse variable

For $x \in \mathbb{R} \cup \{0\}$, sufficient statistics $\phi(x) = \{x, -\frac{1}{2}x^2, \delta(x)\}$, natural parameters $\{b, a, \eta\}$. There is a finite probability that $x = 0$. The natural parameter η corresponding to the sufficient statistic $\delta(x)$ is dual to the fraction of zero elements $\kappa = \mathbb{E}\delta(x) = p(x = 0)$. The sparsity $\rho = 1 - \kappa = p(x \neq 0)$ is the fraction of non-zero elements.

$$A[ab\eta] = \ln \left[e^\eta + \int dx e^{-\frac{1}{2}ax^2 + bx} \right] = \eta + \ln(1 + e^\xi) \quad \text{with} \quad \xi = A[ab] - \eta, \quad (137)$$

$$r[ab\eta] = \frac{b}{a} \sigma(\xi), \quad v[ab\eta] = \frac{1}{a} \sigma(\xi) + \frac{b^2}{a^2} \sigma(\xi) \sigma(-\xi), \quad \rho[ab\eta] = \sigma(\xi), \quad (138)$$

where σ is the sigmoid function and the parameter ξ is the sparsity log-odds:

$$\xi = A[ab] - \eta = \ln \frac{\sigma(\xi)}{\sigma(-\xi)} = \ln \frac{\rho}{1 - \rho}. \quad (139)$$

The corresponding exponential family is the Gauss-Bernoulli:

$$p(x|ab\eta) = [1 - \rho] \delta(x) + \rho \mathcal{N}(x|rv) \quad \text{with} \quad r = \frac{b}{a}, \quad v = \frac{1}{a}, \quad \rho = \rho[ab\eta]. \quad (140)$$

B.1.8 Interval variable

For $x \in X$, sufficient statistics $\phi(x) = \{x, -\frac{1}{2}x^2\}$, natural parameters $\{b, a\}$, where $X = [x_{\min}, x_{\max}] \subset \mathbb{R}$ is a real interval. The probability that x belongs to X is equal to:

$$p_X[ab] = \int_X dx \mathcal{N}(x|rv) = \Phi(z_{\max}) - \Phi(z_{\min}), \quad (141)$$

$$z_{\min} = \frac{x_{\min} - r}{\sqrt{v}} = \frac{ax_{\min} - b}{\sqrt{a}}, \quad z_{\max} = \frac{x_{\max} - r}{\sqrt{v}} = \frac{ax_{\max} - b}{\sqrt{a}}, \quad (142)$$

where Φ is the cumulative Normal distribution and z_{\min} and z_{\max} are the z-scores of x_{\min} and x_{\max} for the Normal of mean $r = \frac{b}{a}$ and variance $v = \frac{1}{a}$. Then:

$$A_X[ab] = \ln \int_X dx e^{-\frac{1}{2}ax^2 + bx} = A[ab] + \ln p_X[ab], \quad (143)$$

$$r_X[ab] = \frac{b}{a} - \frac{1}{\sqrt{a}} \frac{\mathcal{N}(z_{\max}) - \mathcal{N}(z_{\min})}{\Phi(z_{\max}) - \Phi(z_{\min})}, \quad (144)$$

$$v_X[ab] = \frac{1}{a} \left\{ 1 - \frac{z_{\max}\mathcal{N}(z_{\max}) - z_{\min}\mathcal{N}(z_{\min})}{\Phi(z_{\max}) - \Phi(z_{\min})} - \left[\frac{\mathcal{N}(z_{\max}) - \mathcal{N}(z_{\min})}{\Phi(z_{\max}) - \Phi(z_{\min})} \right]^2 \right\}. \quad (145)$$

The corresponding exponential family is the truncated Normal distribution:

$$p_X(x|ab) = \frac{1}{p_X[ab]} \mathcal{N}(x|rv) \delta_X(x) \quad \text{with} \quad r = \frac{b}{a}, \quad v = \frac{1}{a}. \quad (146)$$

B.1.9 Positive/negative variable

For $x \in \mathbb{R}_{\pm}$, sufficient statistics $\phi(x) = \{x, -\frac{1}{2}x^2\}$, natural parameters $\{b, a\}$. It's a particular case of the interval variable with $X = \mathbb{R}_{\pm}$.

$$p_{\pm}[ab] = \int_{\mathbb{R}_{\pm}} dx \mathcal{N}(x|ab) = \Phi(z_{\pm}) \quad \text{with} \quad z_{\pm} = \pm \frac{b}{\sqrt{a}}, \quad (147)$$

$$A_{\pm}[ab] = \ln \int_{\mathbb{R}_{\pm}} dx e^{-\frac{1}{2}ax^2 + bx} = A[ab] + \ln p_{\pm}[ab], \quad (148)$$

$$r_{\pm}[ab] = \pm \frac{1}{\sqrt{a}} \left\{ z_{\pm} + \frac{\mathcal{N}(z_{\pm})}{\Phi(z_{\pm})} \right\}, \quad (149)$$

$$v_{\pm}[ab] = \frac{1}{a} \left\{ 1 - \frac{z_{\pm}\mathcal{N}(z_{\pm})}{\Phi(z_{\pm})} - \frac{\mathcal{N}(z_{\pm})^2}{\Phi(z_{\pm})^2} \right\}. \quad (150)$$

The corresponding exponential family is the half Normal:

$$p_{\pm}(x|ab) = \frac{1}{p_{\pm}[ab]} \mathcal{N}(x|rv) \delta(x \in \mathbb{R}_{\pm}) \quad \text{with} \quad r = \frac{b}{a}, \quad v = \frac{1}{a}. \quad (151)$$

B.1.10 Phase (circular) variable

For $x = e^{i\theta_x} \in U(1)$, sufficient statistics $\phi(x) = \{x\}$, natural parameter $\{b\}$. Generally the von Mises distribution on the circle is defined over the angle $\theta_x \in [0, 2\pi[$ but we find it more convenient to define it over the phase $x = e^{i\theta_x} \in U(1) \simeq \mathbb{S}^1$. Then the natural parameter $b = |b|e^{i\theta_b} \in \mathbb{C}$ and:

$$A_{U(1)}[b] = \ln \int_{U(1)} dx e^{b^\top x} = \ln 2\pi I_0(|b|) \quad (152)$$

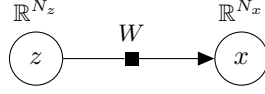
$$r_{U(1)}[b] = \frac{b}{|b|} \frac{I_1(|b|)}{I_0(|b|)}, \quad v_{U(1)}[b] = \frac{1}{2} \left[1 - \frac{I_1(|b|)^2}{I_0(|b|)^2} \right], \quad (153)$$

where I_0 is the modified Bessel function of the first kind. For the natural parameter b , its modulus $|b|$ is called the concentration parameter and is analogous to the precision for a Gaussian, and its angle $\theta_b = \theta_r$ is the circular mean. The corresponding exponential family is the von Mises:

$$p(x|b) = \frac{e^{\kappa \cos(\theta_x - \mu)}}{2\pi I_0(\kappa)} \quad \text{with} \quad \kappa = |b|, \quad \mu = \theta_b. \quad (154)$$

B.2 Linear channels

B.2.1 Generic linear channel



The factor $f(x, z) = p(x|z) = \delta(x - Wz)$ is the deterministic channel $x = Wz$. Unless explicitly specified, we will always consider isotropic Gaussian beliefs on both x and z . The log-partition is given by:

$$A_f[a_{z \rightarrow f} b_{z \rightarrow f} a_{x \rightarrow f} b_{x \rightarrow f}] = \frac{1}{2} b^\top \Sigma b + \frac{1}{2} \ln \det 2\pi \Sigma \quad (155)$$

$$b = b_{z \rightarrow f} + W^\top b_{x \rightarrow f}, \quad a = a_{z \rightarrow f} + a_{x \rightarrow f} W^\top W, \quad \Sigma = a^{-1}. \quad (156)$$

The posterior means and variances are given by:

$$r_z^f = \Sigma b, \quad v_z^f = \mathbb{E}_\lambda \frac{1}{a_{z \rightarrow f} + a_{x \rightarrow f} \lambda}, \quad (157)$$

$$r_x^f = W r_z^f, \quad v_x^f = \frac{1}{\alpha} \mathbb{E}_\lambda \frac{\lambda}{a_{z \rightarrow f} + a_{x \rightarrow f} \lambda}, \quad (158)$$

where $\lambda = \text{Spec } W^\top W$ denotes the spectrum of $W^\top W$ and $\alpha = \frac{N_x}{N_z}$ the aspect ratio of W . There is actually no need to explicitly compute the matrix inverse $\Sigma = a^{-1}$ at each update; it is more numerically efficient to use the SVD decomposition (see Section B.2.6). The variances satisfy:

$$a_{z \rightarrow f} v_z^f + \alpha a_{x \rightarrow f} v_x^f = 1, \quad (159)$$

$$\alpha a_{x \rightarrow f} v_x^f = 1 - a_{z \rightarrow f} v_z^f = n_{\text{eff}}, \quad (160)$$

where $n_{\text{eff}} = \mathbb{E}_\lambda \frac{a_{x \rightarrow f} \lambda}{a_{z \rightarrow f} + a_{x \rightarrow f} \lambda}$ is known as the effective number of parameters in Bayesian linear regression [Bishop, 2006].

B.2.2 Ensemble average

The ensemble average variances are still given by Eqs. (157)-(158). The ensemble average log-partition and the mutual information are equal to

$$A_f[a_f] = \frac{a_{z \rightarrow f} \rho_z + \alpha a_{x \rightarrow f} \rho_x - 1}{2} + \frac{1}{2} \mathbb{E}_\lambda \ln \frac{2\pi}{a_{z \rightarrow f} + a_{x \rightarrow f} \lambda}, \quad (161)$$

$$I_f[a_f] = \frac{1}{2} \mathbb{E}_\lambda \ln \rho_z (a_{z \rightarrow f} + a_{x \rightarrow f} \lambda). \quad (162)$$

From these expressions, it is straightforward to check the variance precision duality:

$$\frac{1}{2} v_z^f = \partial_{a_{z \rightarrow f}} I_f[a_f], \quad \frac{1}{2} \alpha v_x^f = \partial_{a_{x \rightarrow f}} I_f[a_f], \quad (163)$$

as well as the overlap precision duality:

$$\frac{1}{2} m_z^f = \partial_{a_{z \rightarrow f}} A_f[a_f], \quad \frac{1}{2} \alpha m_x^f = \partial_{a_{x \rightarrow f}} A_f[a_f]. \quad (164)$$

B.2.3 Random matrix theory expressions

The posterior variances and the mutual informations are closely related to the following transforms in random matrix theory [Tulino and Verdú, 2004]:

$$\text{Shannon transform} \quad \mathcal{V}(\gamma) = \mathbb{E}_\lambda \ln(1 + \gamma \lambda) \quad (165)$$

$$\eta \text{ transform} \quad \eta(\gamma) = \mathbb{E}_\lambda \frac{1}{1 + \gamma \lambda} \quad (166)$$

$$\text{Stieltjes transform} \quad \mathcal{S}(z) = \mathbb{E}_\lambda \frac{1}{\lambda - z} \quad (167)$$

$$\text{R transform} \quad R(s) = \mathcal{S}^{-1}(-s) - \frac{1}{s} \quad (168)$$

where \mathcal{S}^{-1} denotes the functional inverse of \mathcal{S} . Following [Reeves \[2017\]](#) let's introduce the integrated R-transform and its Legendre transform

$$J(t) = \frac{1}{2} \int_0^t dz R(-z), \quad J^*(u) = \sup_t J(t) - \frac{1}{2} ut. \quad (169)$$

Using the identities [\[Tulino and Verdú, 2004\]](#)

$$\gamma \frac{d}{d\gamma} \mathcal{V}(\gamma) = 1 - \eta(\gamma) = -\phi R(\phi) \quad \text{with } \phi = -\gamma \eta(\gamma), \quad (170)$$

it can be shown that:

$$a_{z \rightarrow f} v_z^f = \eta(\gamma) \quad \text{with } \gamma = \frac{a_{x \rightarrow f}}{a_{z \rightarrow f}}, \quad (171)$$

$$u = \frac{\alpha v_x^f}{v_z^f} = R(\phi), \quad (172)$$

$$I_f[a_f] = \frac{1}{2} \ln \rho_z a_{z \rightarrow f} + \frac{1}{2} \mathcal{V}(\gamma), \quad (173)$$

$$I_f^*[v_f] = J^*(u) + I_z^*[v_z]. \quad (174)$$

The last equation is the same as [\[Reeves, 2017\]](#). When the matrix W belongs to an ensemble for which the limiting spectral density of $W^\top W$ is known³ the transforms above and therefore the variances and mutual informations can be derived analytically, leading to the S-AMP approach [\[Çakmak et al., 2014, 2016\]](#).

B.2.4 Rotation channel

If $W = R$ is a rotation, then $v_z^f = v_x^f = \frac{1}{\alpha}$ and $I_f[a_f] = \frac{1}{2} \ln \rho_z a$ with $a = a_{z \rightarrow f} + a_{x \rightarrow f}$. Besides the forward $f \rightarrow x$ and backward $f \rightarrow z$ updates are simple rotations in parameter space:

$$a_{f \rightarrow x}^{\text{new}} = a_{z \rightarrow f}, \quad b_{f \rightarrow x}^{\text{new}} = R b_{z \rightarrow f}, \quad (175)$$

$$a_{f \rightarrow z}^{\text{new}} = a_{x \rightarrow f}, \quad b_{f \rightarrow z}^{\text{new}} = R^\top b_{x \rightarrow f}. \quad (176)$$

B.2.5 Scaling channel

When the weight matrix $W = S$ is a diagonal $N_x \times N_z$ matrix, the eigenvalue distribution is equal to $\lambda = S^\top S$ and the posterior mean and variances are given by:

$$r_z^f = \frac{b_{z \rightarrow f} + S^\top b_{x \rightarrow f}}{a_{z \rightarrow f} + a_{x \rightarrow f} \lambda}, \quad v_z^f = \mathbb{E}_\lambda \frac{1}{a_{z \rightarrow f} + a_{x \rightarrow f} \lambda}, \quad (177)$$

$$r_x^f = S r_z^f, \quad v_x^f = \frac{1}{\alpha} \mathbb{E}_\lambda \frac{\lambda}{a_{z \rightarrow f} + a_{x \rightarrow f} \lambda}. \quad (178)$$

In particular, for out-of-rank components, the posterior mean r_z^f is set to the prior and the posterior mean r_x^f is set to zero:

$$\text{if } R < i \leq N_z \quad r_z^{f(i)} = \frac{b_{z \rightarrow f}^{(i)}}{a_{z \rightarrow f}}, \quad (179)$$

$$\text{if } R < i \leq N_x \quad r_x^{f(i)} = 0. \quad (180)$$

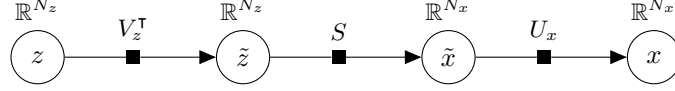
³For instance if W has iid entries of mean 0 and variance of order $\frac{1}{N_z}$, the limiting spectral density of $W^\top W$ is the Marcenko Pastur law

B.2.6 SVD decomposition

As proposed by [Rangan et al. \[2017\]](#) for VAMP, it is more efficient to precompute the SVD decomposition:

$$W = U_x S V_z^\top, U_x \in O(N_x), V_z \in O(N_z), S \in \mathbb{R}^{N_x \times N_z} \text{ diagonal.} \quad (181)$$

The eigenvalue distribution of $W^\top W$ is equal to $\lambda = S^\top S$. Then the EP updates for W are equivalent to the composition of a rotation V_z^\top in z -space, a scaling S that projects z into the x space and a rotation U_x in x -space.



These updates are only rotations or element-wise scaling and are thus considerably faster than solving $ar_z^f = b$ or even worse computing the inverse $\Sigma = a^{-1}$ at each update. It comes at the expense of computing the SVD decomposition of W , but this only needs to be done once.

B.2.7 Complex linear channel

The real linear channel can be easily extended to the complex linear channel $x = Wz$ with $x \in \mathbb{C}^{N_x}$, $z \in \mathbb{C}^{N_z}$ and $W \in \mathbb{C}^{N_x \times N_z}$ and $\lambda = \text{Spec } W^\dagger W$.

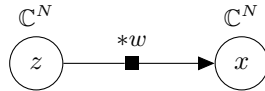
B.2.8 Unitary channel

When $W = U$ is unitary, for instance when $W = \mathcal{F}$ is the discrete Fourier transform (DFT), then $v_z^f = v_x^f = \frac{1}{a}$ and $I_f[a_f] = \frac{1}{2} \ln \rho_z a$ with $a = a_{z \rightarrow f} + a_{x \rightarrow f}$. Besides the forward $f \rightarrow x$ and backward $f \rightarrow z$ updates are simple unitary transforms in parameter space:

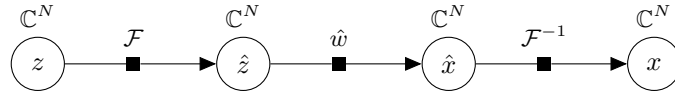
$$a_{f \rightarrow x}^{\text{new}} = a_{z \rightarrow f}, \quad b_{f \rightarrow x}^{\text{new}} = U b_{z \rightarrow f}, \quad (182)$$

$$a_{f \rightarrow z}^{\text{new}} = a_{x \rightarrow f}, \quad b_{f \rightarrow z}^{\text{new}} = U^\dagger b_{x \rightarrow f}. \quad (183)$$

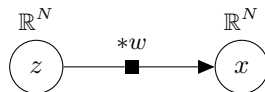
B.2.9 Convolution channel (complex)



The convolution channel $x = w * z$ with convolution weights $w \in \mathbb{C}^N$ is a complex linear channel $x = Wz$ with $N_z = N_x = N$. It is equivalent to the composition of a discrete Fourier transform (DFT) \mathcal{F} for z , a multiplication by $\hat{w} = \mathcal{F}w \in \mathbb{C}^N$, and an inverse DFT \mathcal{F}^{-1} for x . The eigenvalue distribution of $W^\dagger W$ is equal to $\lambda = \hat{w}^\dagger \hat{w} = |w|^2$.

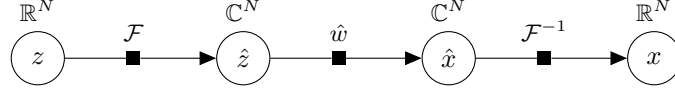


B.2.10 Convolution channel (real)



The convolution channel $x = w * z$ with convolution weights $w \in \mathbb{R}^N$ is a real linear channel $x = Wz$ with $N_z = N_x = N$. It is equivalent to the composition of a discrete Fourier transform (DFT) \mathcal{F} for z , a

multiplication by $\hat{w} = \mathcal{F}w \in \mathbb{C}^N$, and an inverse DFT \mathcal{F}^{-1} for x . The eigenvalue distribution of $W^\top W$ is equal to $\lambda = \hat{w}^\dagger \hat{w} = |\hat{w}|^2$.



B.2.11 Full covariance beliefs

In this subsection we will consider the linear channel $x = Wz$ with full covariance beliefs on x and z , meaning that the precisions $a_{z \rightarrow f}$ and $a_{x \rightarrow f}$ are matrices. The log-partition is given by:

$$A_f[a_{z \rightarrow f} b_{z \rightarrow f} a_{x \rightarrow f} b_{x \rightarrow f}] = \frac{1}{2} b^\top \Sigma b + \frac{1}{2} \ln \det 2\pi \Sigma \quad (184)$$

$$b = b_{z \rightarrow f} + W^\top b_{x \rightarrow f}, \quad a = a_{z \rightarrow f} + W^\top a_{x \rightarrow f} W, \quad \Sigma = a^{-1}. \quad (185)$$

The posterior mean and covariance are given by:

$$r_z^f = \Sigma b, \quad \Sigma_z^f = \Sigma, \quad (186)$$

$$r_x^f = W r_z^f, \quad \Sigma_x^f = W \Sigma W^\top, \quad (187)$$

We have $a_z^f = a$ and $b_z^f = b$ so the backward $f \rightarrow z$ update is simply given by:

$$a_{f \rightarrow z}^{\text{new}} = W^\top a_{x \rightarrow f} W, \quad b_{f \rightarrow z}^{\text{new}} = W^\top b_{x \rightarrow f} \quad (188)$$

We have:

$$a_x^f = (W \Sigma W^\top)^{-1} = a_{x \rightarrow f} + (W a_{z \rightarrow f}^{-1} W^\top)^{-1} \quad (189)$$

$$b_x^f = (W \Sigma W^\top)^{-1} W \Sigma b = b_{x \rightarrow f} + (W \Sigma W^\top)^{-1} W \Sigma b_{z \rightarrow f} \quad (190)$$

The RHS of Eq (190) follows directly from the definition of b . We can obtain the RHS of Eq (189) by two applications of the Woodbury identity. Using the mean and covariance of the $z \rightarrow f$ and $f \rightarrow x$ messages:

$$\Sigma_{z \rightarrow f} = a_{z \rightarrow f}^{-1}, \quad r_{z \rightarrow f} = a_{z \rightarrow f}^{-1} b_{z \rightarrow f} \quad (191)$$

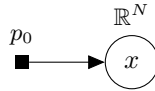
$$\Sigma_{f \rightarrow x} = a_{f \rightarrow x}^{-1}, \quad r_{f \rightarrow x} = a_{f \rightarrow x}^{-1} b_{f \rightarrow x} \quad (192)$$

we can write the forward $f \rightarrow x$ update as:

$$\Sigma_{f \rightarrow x}^{\text{new}} = W \Sigma_{z \rightarrow f} W^\top, \quad r_{f \rightarrow x}^{\text{new}} = W r_{z \rightarrow f}. \quad (193)$$

B.3 Separable priors

B.3.1 Generic separable prior



Let $f(x) = p_0(x) = \prod_{i=1}^N p_0(x^{(i)})$ be a separable prior over $x \in \mathbb{R}^N$. The log-partition, posterior mean and variance are given by:

$$A_f[a_{x \rightarrow f} b_{x \rightarrow f}] = \sum_{i=1}^N A_f[a_{x \rightarrow f} b_{x \rightarrow f}^{(i)}], \quad (194)$$

$$r_x^{f(i)}[a_{x \rightarrow f} b_{x \rightarrow f}] = r_x^f[a_{x \rightarrow f} b_{x \rightarrow f}^{(i)}], \quad (195)$$

$$v_x^f[a_{x \rightarrow f} b_{x \rightarrow f}] = \frac{1}{N} \sum_{i=1}^N v_x^f[a_{x \rightarrow f} b_{x \rightarrow f}^{(i)}]. \quad (196)$$

where on the RHS the same quantities are defined over scalar $b_{x \rightarrow f}^{(i)} \in \mathbb{R}$. In the remainder we will only derive the scalar case, as it can be straightforwardly extended to the high dimensional counterpart through Eqs. (194)-(196). For a large class of priors that we call natural priors we can derive closed-form expressions for the log-partition, mean and variance as shown in Section B.3.3; familiar examples include the Gaussian, binary, Gauss-Bernoulli, and positive priors.

B.3.2 Ensemble average

The ensemble average variance and log-partition are given by:

$$v_x^f[a_{x \rightarrow f}] = \int db_{x \rightarrow f} p(b_{x \rightarrow f} | a_{x \rightarrow f}) v_x^f[a_{x \rightarrow f} b_{x \rightarrow f}], \quad (197)$$

$$A_f[a_{x \rightarrow f}] = \int db_{x \rightarrow f} p(b_{x \rightarrow f} | a_{x \rightarrow f}) A_f[a_{x \rightarrow f} b_{x \rightarrow f}], \quad (198)$$

$$\text{with } p(b_{x \rightarrow f} | a_{x \rightarrow f}) = \mathcal{N}(b_{x \rightarrow f} | 0, a_{x \rightarrow f}) Z_f[a_{x \rightarrow f} b_{x \rightarrow f}]. \quad (199)$$

where the integration is taken over scalar $b_{x \rightarrow f} \in \mathbb{R}$ and $Z_f = e^{A_f}$ is the scalar partition function. The relationship between the mutual information and the log-partition now reads:

$$I_f[a_{x \rightarrow f}] = \frac{1}{2} a_{x \rightarrow f} \rho_x - A_f[a_{x \rightarrow f}]. \quad (200)$$

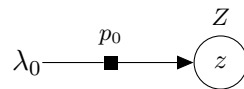
The variance-precision duality and the overlap-precision duality now simply read:

$$\frac{1}{2} v_x^f = \partial_{a_{x \rightarrow f}} I_f[a_{x \rightarrow f}], \quad \frac{1}{2} m_x^f = \partial_{a_{x \rightarrow f}} A_f[a_{x \rightarrow f}]. \quad (201)$$

B.3.3 Natural prior

Let z be a variable of base space Z , with sufficient statistics $\phi(z)$ and associated natural parameters λ_z . Several examples of variable types are presented in Section B.1 such as the real, binary, sparse and positive variable. A natural prior over the variable z is an exponential family distribution $p_0(z) = p(z | \lambda_0) = e^{\lambda_0^T \phi(z) - A_z[\lambda_0]}$ with a given natural parameter λ_0 .

Variable z belief Let the factor $f(z) = p_0(z) = p(z | \lambda_0)$ be a natural prior. Let us first consider the corresponding module with variable z belief.



The log-partition and moment function are given by:

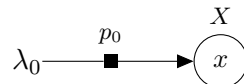
$$A_f[\lambda_{z \rightarrow f}] = A_z[\lambda_{z \rightarrow f} + \lambda_0] - A_z[\lambda_0], \quad (202)$$

$$\mu_z^f[\lambda_{z \rightarrow f}] = \mu_z[\lambda_{z \rightarrow f} + \lambda_0], \quad (203)$$

where $A_z[\lambda]$ and $\mu_z[\lambda]$ denotes the log-partition and moment function of the variable z . The $f \rightarrow z$ update is the constant message:

$$\lambda_{f \rightarrow z}^{\text{new}} = \lambda_0. \quad (204)$$

Variable x belief Let x be a variable of different type than z , with base space X and sufficient statistics $\phi(x)$ and associated natural parameters λ_x . We still consider the same factor $f(x) = p_0(x) = p(x | \lambda_0)$ which is a natural prior in the z variable, but we derive the corresponding module using a variable x belief.



This is meaningful only if we can inject $Z \hookrightarrow X$. We denote by $\phi^{(0)}$, $\phi^{(1)}$ and $\phi^{(2)}$ the set of sufficient statistics common to x and z , specific to z and specific to x respectively. We will assume that the sufficient statistics $\phi^{(2)}$ specific to x are constant on Z :

$$\phi^{(2)}(z) = \mu_Z^{(2)} \quad \text{for all } z \in Z. \quad (205)$$

Then the log-partition and moment function are given by:

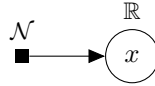
$$A_f[\lambda_{x \rightarrow f}] = A_z[\lambda_{z \rightarrow f} + \lambda_0] - A_z[\lambda_0] + \lambda_{x \rightarrow f}^T \mu_Z^{(2)}, \quad (206)$$

$$\mu_x^{f(0)}[\lambda_{x \rightarrow f}] = \mu_z^{(0)}[\lambda_{z \rightarrow f} + \lambda_0], \quad \mu_x^{f(2)}[\lambda_{x \rightarrow f}] = \mu_Z^{(2)} \quad (207)$$

with $\lambda_{z \rightarrow f}^{(0)} = \lambda_{x \rightarrow f}^{(0)}$ and $\lambda_{z \rightarrow f}^{(1)} = 0$.

Isotropic Gaussian belief To derive the isotropic Gaussian belief modules, we take x to be a real variable that is $X = \mathbb{R}$ and $\phi(x) = \{x, -\frac{1}{2}x^2\}$ and associated natural parameters b_x and a_x . When z is a real, binary, sparse, and interval variable we obtain respectively the Gaussian, binary, Gauss-Bernoulli and truncated Normal prior as detailed in the next subsections.

B.3.4 Gaussian prior



The factor $f(x) = p(x|a_0b_0) = \mathcal{N}(x|r_0v_0)$ is the Normal prior with natural parameters $a_0 = \frac{1}{v_0}$ and $b_0 = \frac{r_0}{v_0}$. The Normal prior corresponds to the natural prior for the real variable $x \in \mathbb{R}$. According to Section B.3.3 the log-partition is given by:

$$A_f[a_{x \rightarrow f}b_{x \rightarrow f}] = A[ab] - A[a_0b_0] \quad \text{with} \quad a = a_{x \rightarrow f} + a_0, \quad b = b_{x \rightarrow f} + b_0, \quad (208)$$

where $A[ab]$ is the log-partition of a real variable, see Section B.1.5. The posterior mean and variance are given by:

$$r_x^f = \frac{b}{a}, \quad v_x^f = \frac{1}{a}, \quad (209)$$

leading to the constant $f \rightarrow x$ update:

$$a_{f \rightarrow x}^{\text{new}} = a_0, \quad b_{f \rightarrow x}^{\text{new}} = b_0. \quad (210)$$

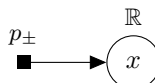
The ensemble average variance is directly given by $v_x^f = \frac{1}{a}$. The ensemble average log-partition and the mutual information are given by:

$$A_f[a_{x \rightarrow f}] = \frac{a_{x \rightarrow f} \rho_x}{2} + \frac{1}{2} \ln \frac{a_0}{a}, \quad I_f[a_{x \rightarrow f}] = \frac{1}{2} \ln v_0 a. \quad (211)$$

From these expressions, it is straightforward to check the variance precision duality and overlap precision duality:

$$\frac{1}{2}v_x^f = \partial_{a_{x \rightarrow f}} I_f[a_{x \rightarrow f}], \quad \frac{1}{2}m_x^f = \partial_{a_{x \rightarrow f}} A_f[a_{x \rightarrow f}]. \quad (212)$$

B.3.5 Binary prior



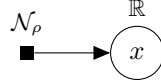
The factor $f(x) = p(x|b_0) = p_+\delta_{+1}(x) + p_-\delta_{-1}(x)$ is the binary prior with natural parameter $b_0 = \frac{1}{2} \ln \frac{p_+}{p_-}$. The binary prior corresponds to the natural prior for the binary variable $z \in \pm$. According to Section B.3.3 the log-partition, posterior mean and variance are given by:

$$A_f[a_{x \rightarrow f} b_{x \rightarrow f}] = A[b] - A[b_0] - \frac{a_{x \rightarrow f}}{2} \quad \text{with} \quad b = b_0 + b_{x \rightarrow f}, \quad (213)$$

$$r_x^f = r[b], \quad v_x^f = v[b], \quad (214)$$

where $A[b]$, $r[b]$ and $v[b]$ denote the log-partition, mean and variance of a binary variable, see Section B.1.6.

B.3.6 Sparse prior



The factor $f(x) = p(x|a_0 b_0 \eta_0) = [1 - \rho_0] \delta_0(x) + \rho_0 \mathcal{N}(x|r_0 v_0)$ is the Gauss-Bernoulli prior with natural parameters $a_0 = \frac{1}{v_0}$, $b_0 = \frac{r_0}{v_0}$ and $\eta_0 = A[a_0 b_0] - \ln \frac{\rho_0}{1-\rho_0}$ where $A[ab] = \frac{b^2}{2a} + \frac{1}{2} \ln \frac{2\pi}{a}$ is the log-partition of a real variable. The Gauss-Bernoulli prior corresponds to the natural prior for the sparse variable $z \in \mathbb{R} \cup \{0\}$. According to Section B.3.3 the log-partition, posterior mean and variance are given by:

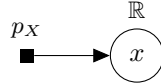
$$A_f[a_{x \rightarrow f} b_{x \rightarrow f}] = A[ab\eta_0] - A[a_0 b_0 \eta_0] \quad \text{with} \quad a = a_0 + a_{x \rightarrow f}, \quad b = b_0 + b_{x \rightarrow f}, \quad (215)$$

$$r_x^f = r[ab\eta_0], \quad v_x^f = v[ab\eta_0], \quad (216)$$

where $A[ab\eta]$, $r[ab\eta]$ and $v[ab\eta]$ denote the log-partition, mean and variance of a sparse variable, see Section B.1.7. Also the sparsity of x is equal to $\rho_x^f = \rho[ab\eta_0]$.

B.3.7 Interval prior

Let $X \subset \mathbb{R}$ denotes any real interval, for example $X = \mathbb{R}_+$ for a positive prior.



The factor $f(x) = p_X(x|a_0 b_0) = \frac{1}{p_X[a_0 b_0]} \mathcal{N}(x|r_0 v_0) \delta_X(x)$ is the truncated Normal prior with natural parameters $a_0 = \frac{1}{v_0}$ and $b_0 = \frac{r_0}{v_0}$. The truncated Normal corresponds to the natural prior for the interval variable $z \in X$. According to Section B.3.3 the log-partition, posterior mean and variance are given by:

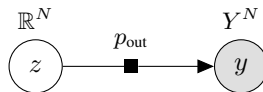
$$A_f[a_{x \rightarrow f} b_{x \rightarrow f}] = A_X[ab] - A_X[a_0 b_0] \quad \text{with} \quad a = a_0 + a_{x \rightarrow f}, \quad b = b_0 + b_{x \rightarrow f}, \quad (217)$$

$$r_x^f = r_X[ab], \quad v_x^f = v_X[ab] \quad (218)$$

where $A_X[ab]$, $r_X[ab]$ and $v_X[ab]$ denote the log-partition, mean and variance of a interval X variable, see Section B.1.8.

B.4 Separable likelihoods

B.4.1 Generic separable likelihood



Let $f(x) = p_{\text{out}}(y|z) = \prod_{i=1}^N p_{\text{out}}(y^{(i)}|x^{(i)})$ be a separable likelihood over $z \in \mathbb{R}^N$ with observed $y \in Y^N$. The log-partition, posterior means and variances are given by:

$$A_f[a_{z \rightarrow f} b_{z \rightarrow f}; y] = \sum_{i=1}^N A_f[a_{z \rightarrow f} b_{z \rightarrow f}^{(i)}; y^{(i)}], \quad (219)$$

$$r_z^{f(i)}[a_{z \rightarrow f} b_{z \rightarrow f}; y] = r_z^f[a_{z \rightarrow f} b_{z \rightarrow f}^{(i)}; y^{(i)}], \quad (220)$$

$$v_x^f[a_{x \rightarrow f} b_{x \rightarrow f}; y] = \frac{1}{N} \sum_{i=1}^N v_x^f[a_{x \rightarrow f} b_{x \rightarrow f}^{(i)}; y^{(i)}]. \quad (221)$$

where on the RHS the same quantities are defined over scalar $b_{x \rightarrow f}^{(i)} \in \mathbb{R}$ and $y^{(i)} \in \mathbb{R}$. In the remainder we will only derive the scalar case, as it can be straightforwardly extended to the high dimensional counterpart through Eqs. (219)-(221).

B.4.2 Ensemble average

The ensemble average variance and log-partition are given by:

$$v_z^f[a_{z \rightarrow f}] = \int dy db_{z \rightarrow f} p(y, b_{z \rightarrow f} | a_{z \rightarrow f}) v_z^f[a_{z \rightarrow f} b_{z \rightarrow f}; y], \quad (222)$$

$$A_f[a_{z \rightarrow f}] = \int dy db_{z \rightarrow f} p(y, b_{z \rightarrow f} | a_{z \rightarrow f}) A_f[a_{z \rightarrow f} b_{z \rightarrow f}; y], \quad (223)$$

$$\text{with } p(y, b_{z \rightarrow f} | a_{z \rightarrow f}) = \mathcal{N}(b_{z \rightarrow f} | 0, a_{z \rightarrow f} - 1/\rho_z) Z_f[a_{z \rightarrow f} b_{z \rightarrow f}; y] \frac{1}{\sqrt{2\pi\rho_z}} \quad (224)$$

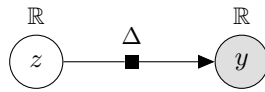
where the integration is taken over scalar $b_{z \rightarrow f} \in \mathbb{R}$ and $y \in \mathbb{R}$ and $Z_f = e^{A_f}$ is the scalar partition function. The relationship between the mutual information and the log-partition now reads:

$$I_f[a_{z \rightarrow f}] = \frac{1}{2} a_{z \rightarrow f} \rho_z - A_f[a_{z \rightarrow f}] + \frac{1}{2} \ln \frac{2\pi\rho_z}{e}. \quad (225)$$

The variance-precision duality and the overlap-precision duality now simply read:

$$\frac{1}{2} v_z^f = \partial_{a_{z \rightarrow f}} I_f[a_{z \rightarrow f}], \quad \frac{1}{2} m_z^f = \partial_{a_{z \rightarrow f}} A_f[a_{z \rightarrow f}]. \quad (226)$$

B.4.3 Gaussian likelihood



The factor $f(z) = p(y|z) = \mathcal{N}(y|z\Delta)$ is the Gaussian likelihood with noise variance Δ and observed y . The log-partition is given by:

$$A_f[a_{z \rightarrow f} b_{z \rightarrow f}; y] = A[ab] - A[a_y b_y], \quad (227)$$

$$a_y = \frac{1}{\Delta}, \quad b_y = \frac{y}{\Delta}, \quad a = a_{z \rightarrow f} + a_y, \quad b = b_{z \rightarrow f} + b_y, \quad (228)$$

where $A[ab]$ denotes the log-partition of a real variable, see Section B.1.5. The posterior mean and variance are given by:

$$r_z^f = \frac{b}{a}, \quad v_z^f = \frac{1}{a}, \quad (229)$$

leading to the constant $f \rightarrow z$ update:

$$a_{f \rightarrow z}^{\text{new}} = a_y, \quad b_{f \rightarrow z}^{\text{new}} = b_y. \quad (230)$$

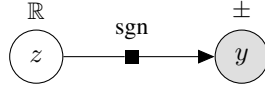
The ensemble average variance is directly given by $v_z^f = \frac{1}{a}$. The ensemble average log-partition and the mutual information are given by:

$$A_f[a_{z \rightarrow f}] = \frac{a_{z \rightarrow f} \rho_z}{2} - 1 + \frac{1}{2} \ln \frac{a_y}{a}, \quad I_f[a_{z \rightarrow f}] = \frac{1}{2} \ln \rho_z a + \frac{1}{2} \ln 2\pi e \Delta. \quad (231)$$

From these expressions, it is straightforward to check the variance precision duality and overlap precision duality:

$$\frac{1}{2} v_z^f = \partial_{a_{z \rightarrow f}} I_f[a_{z \rightarrow f}], \quad \frac{1}{2} m_z^f = \partial_{a_{z \rightarrow f}} A_f[a_{z \rightarrow f}]. \quad (232)$$

B.4.4 Sgn likelihood



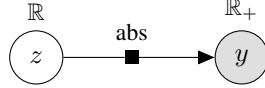
The factor $f(z) = p(y|z) = \delta(y - \text{sgn}(z))$ is the deterministic likelihood $y = \text{sgn}(z) \in \pm$. The log-partition, posterior mean and variance are given by:

$$A_f[a_{z \rightarrow f} b_{z \rightarrow f}; y] = A_y[a_{z \rightarrow f} b_{z \rightarrow f}], \quad (233)$$

$$r_z^f = r_y[a_{z \rightarrow f} b_{z \rightarrow f}], \quad v_z^f = v_y[a_{z \rightarrow f} b_{z \rightarrow f}], \quad (234)$$

where $A_{\pm}[ab]$, $r_{\pm}[ab]$ and $v_{\pm}[ab]$ denote the log-partition, mean and variance of a positive/negative variable, see Section B.1.9.

B.4.5 Abs likelihood



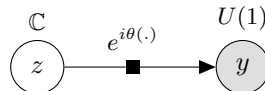
The factor $f(z) = p(y|z) = \delta(y - \text{abs}(z))$ is the deterministic likelihood $y = \text{abs}(z) \in \mathbb{R}_+$. The log-partition, posterior mean and variance are given by:

$$A_f[a_{z \rightarrow f} b_{z \rightarrow f}; y] = -\frac{a_{z \rightarrow f} y^2}{2} + A[b] \quad \text{with} \quad b = y b_{z \rightarrow f}, \quad (235)$$

$$r_z^f = y r[b], \quad v_z^f = y^2 v[b], \quad (236)$$

where $A[b]$, $r[b]$ and $v[b]$ denote the log-partition, mean and variance of a binary variable, see Section B.1.6.

B.4.6 Phase likelihood



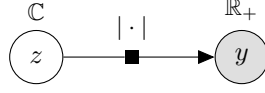
The factor $f(z) = p(y|z) = \delta(y - e^{i\theta(z)})$ is the deterministic likelihood $y = e^{i\theta(z)} \in U(1)$. The log-partition, posterior mean and variance are given by:

$$A_f[a_{z \rightarrow f} b_{z \rightarrow f}; y] = A_+[a_{z \rightarrow f} b] \quad \text{with} \quad b = y^\top b_{z \rightarrow f}, \quad (237)$$

$$r_z^f = y r_+[a_{z \rightarrow f} b], \quad v_z^f = \frac{1}{2} v_+[a_{z \rightarrow f} b], \quad (238)$$

where $A_+[ab]$, $r_+[ab]$ and $v_+[ab]$ denote the log-partition, mean and variance of a positive variable, see Section B.1.9. The $\frac{1}{2}$ factor in the variance comes from the average over the real and imaginary parts.

B.4.7 Modulus likelihood



The factor $f(z) = p(y|z) = \delta(y - |z|)$ is the deterministic likelihood $y = |z| \in \mathbb{R}_+$. The log-partition, posterior mean and variance are given by:

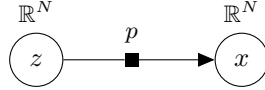
$$A_f[a_{z \rightarrow f} b_{z \rightarrow f}; y] = -\frac{a_{z \rightarrow f} y^2}{2} + \ln y + A_{U(1)}[b] \quad \text{with} \quad b = y b_{z \rightarrow f}, \quad (239)$$

$$r_z^f = y r_{U(1)}[b], \quad v_z^f = y^2 v_{U(1)}[b], \quad (240)$$

where $A_{U(1)}[b]$, $r_{U(1)}[b]$ and $v_{U(1)}[b]$ denote the log-partition, mean and variance of a phase variable, see Section B.1.10.

B.5 Separable channels

B.5.1 Generic separable channel



Let $f(x, z) = p(x|z) = \prod_{i=1}^N p(x^{(i)}|z^{(i)})$ be a separable channel with input $z \in \mathbb{R}^N$ and output $x \in \mathbb{R}^N$. The log-partition, posterior means and variances are given by:

$$A_f[a_f b_f] = \sum_{i=1}^N A_f[a_f b_f^{(i)}], \quad (241)$$

$$r_x^{f(i)}[a_f b_f] = r_x^f[a_f b_f^{(i)}], \quad r_z^{f(i)}[a_f b_f] = r_z^f[a_f b_f^{(i)}], \quad (242)$$

$$v_x^f[a_f b_f] = \frac{1}{N} \sum_{i=1}^N v_x^f[a_f b_f^{(i)}], \quad v_z^f[a_f b_f] = \frac{1}{N} \sum_{i=1}^N v_z^f[a_f b_f^{(i)}]. \quad (243)$$

where on the RHS the same quantities are defined over scalar $b_{x \rightarrow f}^{(i)} \in \mathbb{R}$ and $b_{z \rightarrow f}^{(i)} \in \mathbb{R}$. In the remainder we will only derive the scalar case, as it can be straightforwardly extended to the high dimensional counterpart through Eqs. (241)-(243).

B.5.2 Ensemble average

The ensemble average variance and log-partition are given by:

$$v_x^f[a_f] = \int db_f p(b_f|a_f) v_x^f[a_f b_f], \quad (244)$$

$$v_z^f[a_f] = \int db_f p(b_f|a_f) v_z^f[a_f b_f], \quad (245)$$

$$A_f[a_f] = \int db_f p(b_f|a_f) A_f[a_f b_f], \quad (246)$$

$$\text{with } p(b_f|a_f) = \mathcal{N}(b_{x \rightarrow f}|0, a_{x \rightarrow f}) \mathcal{N}(b_{z \rightarrow f}|0, a_{z \rightarrow f} - 1/\rho_z) Z_f[a_f b_f] \frac{1}{\sqrt{2\pi\rho_z}}. \quad (247)$$

where the integration is taken over scalar $b_{z \rightarrow f} \in \mathbb{R}$ and $b_{x \rightarrow f} \in \mathbb{R}$ and $Z_f = e^{A_f}$ is the scalar partition function. The relationship between the mutual information and the log-partition now reads:

$$I_f[a_f] = \frac{1}{2}(a_{x \rightarrow f} \rho_x + a_{z \rightarrow f} \rho_z) - A_f[a_f] + \frac{1}{2} \ln \frac{2\pi\rho_z}{e}. \quad (248)$$

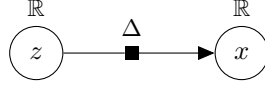
The variance precision duality now simply reads:

$$\frac{1}{2}v_z^f = \partial_{a_{z \rightarrow f}} I_f[a_f], \quad \frac{1}{2}v_x^f = \partial_{a_{x \rightarrow f}} I_f[a_f], \quad (249)$$

and the overlap precision duality reads:

$$\frac{1}{2}m_z^f = \partial_{a_{z \rightarrow f}} A_f[a_f], \quad \frac{1}{2}m_x^f = \partial_{a_{x \rightarrow f}} A_f[a_f]. \quad (250)$$

B.5.3 Gaussian noise channel



The factor $f(x, z) = p(x|z) = \mathcal{N}(x|z\Delta)$ is the additive Gaussian noise channel $x = z + \sqrt{\Delta}\xi$ with variance Δ and precision $a_\Delta = \Delta^{-1}$. The log-partition is given by:

$$A_f[a_f b_f] = \frac{1}{2}b^\top \Sigma b + \frac{1}{2} \ln \det 2\pi \Sigma - \frac{1}{2} \ln 2\pi \Delta, \quad (251)$$

$$b = \begin{bmatrix} b_{z \rightarrow f} \\ b_{x \rightarrow f} \end{bmatrix}, \quad A = \begin{bmatrix} a_\Delta + a_{z \rightarrow f} & -a_\Delta \\ -a_\Delta & a_\Delta + a_{x \rightarrow f} \end{bmatrix}, \quad \Sigma = A^{-1}. \quad (252)$$

The posterior mean and variance are given by:

$$v_z^f = \frac{a_\Delta + a_{x \rightarrow \Delta}}{a_\Delta a}, \quad r_z^f = v_z^f \left[b_{z \rightarrow f} + \frac{a_\Delta b_{x \rightarrow f}}{a_\Delta + a_{x \rightarrow f}} \right], \quad (253)$$

$$v_x^f = \frac{a_\Delta + a_{z \rightarrow \Delta}}{a_\Delta a}, \quad r_x^f = v_x^f \left[b_{x \rightarrow f} + \frac{a_\Delta b_{z \rightarrow f}}{a_\Delta + a_{z \rightarrow f}} \right], \quad (254)$$

$$\text{with } a = a_{x \rightarrow f} + a_{z \rightarrow f} + \frac{a_{x \rightarrow f} a_{z \rightarrow f}}{a_\Delta}. \quad (255)$$

We therefore have:

$$a_z^f = a_{z \rightarrow f} + \frac{a_\Delta a_{x \rightarrow f}}{a_\Delta + a_{x \rightarrow f}}, \quad b_z^f = \left[b_{z \rightarrow f} + \frac{a_\Delta b_{x \rightarrow f}}{a_\Delta + a_{x \rightarrow f}} \right], \quad (256)$$

$$a_x^f = a_{x \rightarrow f} + \frac{a_\Delta a_{z \rightarrow f}}{a_\Delta + a_{z \rightarrow f}}, \quad b_x^f = \left[b_{x \rightarrow f} + \frac{a_\Delta b_{z \rightarrow f}}{a_\Delta + a_{z \rightarrow f}} \right]. \quad (257)$$

leading to the backward $f \rightarrow z$ and forward $f \rightarrow x$ updates:

$$a_{f \rightarrow z}^{\text{new}} = \frac{a_\Delta}{a_\Delta + a_{x \rightarrow f}} a_{x \rightarrow f}, \quad b_{f \rightarrow z}^{\text{new}} = \frac{a_\Delta}{a_\Delta + a_{x \rightarrow f}} b_{x \rightarrow f}, \quad (258)$$

$$a_{f \rightarrow x}^{\text{new}} = \frac{a_\Delta}{a_\Delta + a_{z \rightarrow f}} a_{z \rightarrow f}, \quad b_{f \rightarrow x}^{\text{new}} = \frac{a_\Delta}{a_\Delta + a_{z \rightarrow f}} b_{z \rightarrow f}. \quad (259)$$

The ensemble average variances are still given by Eqs. (253)-(254). The ensemble average log-partition and the mutual information are given by:

$$A_f[a_f] = \frac{a_{z \rightarrow f} \rho_z + a_{x \rightarrow f} \rho_x - 1}{2} + \frac{1}{2} \ln \frac{2\pi}{a}, \quad I_f[a_f] = \frac{1}{2} \ln \rho_z a. \quad (260)$$

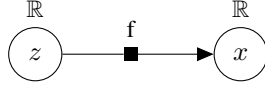
From these expressions, it is straightforward to check the variance precision duality:

$$\frac{1}{2}v_z^f = \partial_{a_{z \rightarrow f}} I_f[a_f], \quad \frac{1}{2}v_x^f = \partial_{a_{x \rightarrow f}} I_f[a_f], \quad (261)$$

as well as the overlap precision duality:

$$\frac{1}{2}m_z^f = \partial_{a_{z \rightarrow f}} A_f[a_f], \quad \frac{1}{2}m_x^f = \partial_{a_{x \rightarrow f}} A_f[a_f]. \quad (262)$$

B.5.4 Piecewise linear activation



Factor $f(x, z) = p(x|z) = \delta(x - f(z))$ is the deterministic channel $x = f(z)$, where we assume the activation to be piecewise linear⁴

$$f(z) = \sum_R \delta_R(z) [x_R + \gamma_R z]. \quad (263)$$

As the real line \mathbb{R} is the disjoint union of the regions R , the factor partition function is simply the sum of the region partition functions:

$$Z_f[a_f b_f] = \sum_R Z_{f,R}[a_f b_f], \quad (264)$$

$$Z_{f,R}[a_f b_f] = \int_R dz e^{-\frac{1}{2} a_{x \rightarrow f} [x_R + \gamma_R z]^2 + b_{x \rightarrow f}^\top [x_R + \gamma_R z] - \frac{1}{2} a_{z \rightarrow f} z^2 + b_{z \rightarrow f}^\top z}. \quad (265)$$

Thus at the factor level, the log-partition, posterior means and variances are given by:

$$A_f[a_f b_f] = \ln \sum_R e^{A_{f,R}[a_f b_f]}, \quad (266)$$

$$r_z^f = \sum_R \sigma_R r_z^R, \quad \sigma = \text{softmax}\{A_{f,R}\}, \quad (267)$$

$$r_x^f = \sum_R \sigma_R r_x^R \quad (268)$$

$$v_z^f = \sum_R \sigma_R v_z^R + \sum_{R < R'} \sigma_R \sigma_{R'} [r_z^R - r_z^{R'}]^2 \quad (269)$$

$$v_x^f = \sum_R \sigma_R v_x^R + \sum_{R < R'} \sigma_R \sigma_{R'} [r_x^R - r_x^{R'}]^2 \quad (270)$$

The corresponding quantities at the linear region level are given by:

$$A_{f,R}[a_f b_f] = -\frac{a_{x \rightarrow f} x_R^2}{2} + b_{x \rightarrow f} x_R + A_R[ab], \quad (271)$$

$$r_z^R = r_R[ab], \quad r_x^R = x_R + \gamma_R r_z^R, \quad (272)$$

$$v_z^R = v_R[ab], \quad v_x^R = \gamma_R^2 v_z^R, \quad (273)$$

$$\text{with } a = a_{z \rightarrow f} + \gamma_R^2 a_{x \rightarrow f}, \quad b = b_{z \rightarrow f} + \gamma_R [b_{x \rightarrow f} - a_{x \rightarrow f} x_R], \quad (274)$$

where $A_R[ab]$, $r_R[ab]$ and $v_R[ab]$ denote the log-partition, mean and variance of an interval R variable, see Section B.1.8.

⁴ ReLU, leaky ReLU, hard tanh, hard sigmoid, sgn and abs are popular examples.

C Proof of overlap/variance precision duality

C.1 Derivative of A_x and I_x

Since $A_x[a_x] = \frac{1}{2}a_x\rho_x - \frac{1}{2} + \frac{1}{2}\ln\frac{2\pi}{a_x}$ and $m_x = \rho_x - v_x$ and $v_x = \frac{1}{a_x}$:

$$\partial_{a_x}A_x = \frac{1}{2}(\rho_x - v_x) = \frac{1}{2}m_x. \quad (275)$$

Since $I_x[a_x] = \frac{1}{2}\ln\rho_x a_x$ and $v_x = \frac{1}{a_x}$:

$$\partial_{a_x}I_x = \frac{1}{2}v_x. \quad (276)$$

C.2 Derivative of A_f and I_f

The ensemble average log-partition can be written as

$$N_f A_f[a_f] = \int db_f p(b_f|a_f) A_f[a_f b_f] \quad (277)$$

where the expectation over b_f is obtained by marginalizing the teacher generative distribution Eq. (71) over x_f and substituting $z_f \rightarrow b_f$:

$$p(b_f|a_f) = \mathcal{N}(b_f^+ | 0, a_f^+) \mathcal{N}(b_f^- | 0, a_f^- - 1/\rho_f^-) Z_f[a_f b_f] \prod_{x \in f_-} \frac{1}{\sqrt{2\pi\rho_x}}. \quad (278)$$

The partition function $Z_f[ab] = \int dx_f f(x_f) e^{-\frac{1}{2}ax_f^\top x_f + b^\top x_f}$, the log-partition $A_f[ab]$ and the normal $\mathcal{N}(b|0, a)$ verify:

$$\partial_a Z_f[ab] = -\frac{1}{2}\partial_b^2 Z_f[ab] \quad (279)$$

$$\partial_b A_f[ab] = r_f[ab] \quad (280)$$

$$\partial_a A_f[ab] = -\frac{1}{2}\{\partial_b^2 A_f[ab] + (\partial_b A_f[ab])^2\} \quad (281)$$

$$\partial_a \mathcal{N}(b|0, a) = \frac{1}{2}\partial_b^2 \mathcal{N}(b|0, a) \quad (282)$$

Using the previous identities and integrating by parts one ultimately finds:

$$N_f \partial_{a_{x \rightarrow f}} A_f[a_f] = \int db_f p(b_f|a_f) \frac{1}{2} \|r_x^f[a_f b_f]\|^2. \quad (283)$$

Or using the self-overlap $q_x^f[a_f] = \mathbb{E} \frac{\|r_x^f\|^2}{N_x}$ and $\alpha_x^f = \frac{N_x}{N_f}$:

$$\partial_{a_{x \rightarrow f}} A_f[a_f] = \frac{1}{2} \alpha_x^f q_x^f[a_f]. \quad (284)$$

Note that the teacher student scenario we are considering is Bayes optimal so $q_x^f = m_x^f = \rho_x - v_x^f$ and therefore:

$$\partial_{a_{x \rightarrow f}} A_f[a_f] = \frac{1}{2} \alpha_x^f m_x^f[a_f]. \quad (285)$$

Since I_f and A_f are related by Eq. (78) and $m_x^f = \rho_x - v_x^f$:

$$\partial_{a_{x \rightarrow f}} I_f = \frac{1}{2} \alpha_x^f \rho_x - \partial_{a_{x \rightarrow f}} A_f = \frac{1}{2} \alpha_x^f (\rho_x - m_x^f) = \frac{1}{2} \alpha_x^f v_x^f. \quad (286)$$

D Proof of Proposition 3

D.1 Minimization of $A^*[\{m_x\}]$

First, minimizing $A^*[m]$ over $m = \{m_x\}$ leads to:

$$0 = \partial_{m_x} A^*[m] = \sum_{f \in x} a_{x \rightarrow f} [m_f] + (1 - n_x) a_x [m_x] \quad (287)$$

which is the precision constraint. The solution is therefore the same as the state evolution fixed point Eq. (98). The same holds for $I^*[v]$ as $A^*[m] = I^*[v]$.

D.2 Stationary point of $A[\{a_x, a_f\}]$

Using the duality between precisions and overlaps:

$$\begin{aligned} \min_m A^*[m] &= \min_m \sum_f \alpha_f A_f^*[m_f] + \sum_x \alpha_x (1 - n_x) A_x^*[m_x] \\ &= \min_m \sum_f \alpha_f \max_{a_f} \left\{ \sum_{x \in f} \frac{1}{2} \alpha_x^f a_{x \rightarrow f} m_x - A_f[a_f] \right\} \\ &\quad + \sum_x \alpha_x \underbrace{(1 - n_x)}_{\leq 0} \max_{a_x} \left\{ \frac{1}{2} a_x m_x - A_x[a_x] \right\} \\ &= \min_m \min_{a_x} \max_{a_f} - \sum_f \alpha_f A_f[a_f] - \sum_x \alpha_x (1 - n_x) A_x[a_x] \\ &\quad + \sum_x \alpha_x m_x \left[\sum_{f \in x} a_{x \rightarrow f} + (1 - n_x) a_x \right] \\ &= \min_{a_x} \max_{a_f} - A[\{a_x, a_f\}] \quad \text{s.t.} \quad (n_x - 1) a_x = \sum_{f \in x} a_{x \rightarrow f}. \end{aligned} \quad (288)$$

As a consistency check, let's derive the solution to Eq. (288). Consider the Lagrangian:

$$\mathcal{L}[\{a_x, a_f, m_x\}] = A[\{a_x, a_f\}] + \frac{1}{2} \sum_x m_x \left[(n_x - 1) a_x - \sum_{f \in x} a_{x \rightarrow f} \right] \quad (289)$$

with Lagrangian multiplier m_x associated to the precision constraint $(n_x - 1) a_x = \sum_{f \in x} a_{x \rightarrow f}$. At a stationary point:

$$\partial_{m_x} \mathcal{L} = 0 \implies (n_x - 1) a_x = \sum_{f \in x} a_{x \rightarrow f} \quad (290)$$

$$\partial_{a_f} \mathcal{L} = 0 \implies m_x = m_x^f[a_f] \quad (291)$$

$$\partial_{a_x} \mathcal{L} = 0 \implies m_x = m_x[a_x] \quad (292)$$

which is the same as the state evolution fixed point Eq. (98). Furthermore the Lagrangian multiplier is the posterior overlap $m_x = m_x^*$.

D.3 Stationary point of $A[\{a_{x \rightarrow f}, a_{f \rightarrow x}\}]$

Finally, the optimization under constraint of $A[\{a_x, a_f\}]$ is equivalent to finding a stationary point of $A[\{a_{f \rightarrow x}, a_{x \rightarrow f}\}]$ without any constraint. Indeed:

$$\partial_{a_{f \rightarrow x}} A = 0 \implies m_x[a_x^f] = m_x[a_x] \implies a_x^f = a_x \quad (293)$$

$$\partial_{a_{x \rightarrow f}} A = 0 \implies m_x^f[a_f] = m_x[a_x^f] \quad (294)$$

which implies the overlap matching:

$$m_x^f[a_f] = m_x[a_x] \quad (295)$$

as well as the precision constraint:

$$\sum_{f \in x} a_{x \rightarrow f} = \sum_{f \in x} (a_x - a_{f \rightarrow x}) = n_x a_x - a_x = (n_x - 1) a_x \quad (296)$$

which again corresponds to the state evolution fixed point Eq. (98).

References

- Benjamin Aubin, Antoine Maillard, Jean Barbier, Florent Krzakala, Nicolas Macris, and Lenka Zdeborová. The committee machine: Computational to statistical gaps in learning a two-layers neural network. In *Advances in Neural Information Processing Systems*, volume 2018-Decem, pages 3223–3234, 2018.
- Benjamin Aubin, Bruno Loureiro, Antoine Baker, Florent Krzakala, and Lenka Zdeborová. Exact asymptotics for phase retrieval and compressed sensing with random generative priors, 2019a.
- Benjamin Aubin, Bruno Loureiro, Antoine Maillard, Florent Krzakala, and Lenka Zdeborová. The spiked matrix model with generative priors. In *Advances in Neural Information Processing Systems 32*, pages 8366–8377. 2019b.
- Jean Barbier, Mohamad Dia, Nicolas Macris, and Florent Krzakala. The mutual information in random linear estimation. In *2016 54th Annual Allerton Conference on Communication, Control, and Computing (Allerton)*, pages 625–632. IEEE, 2016.
- Jean Barbier, Nicolas Macris, Antoine Maillard, and Florent Krzakala. The mutual information in random linear estimation beyond iid matrices. In *2018 IEEE International Symposium on Information Theory (ISIT)*, pages 1390–1394. IEEE, 2018.
- Jean Barbier, Florent Krzakala, Nicolas Macris, Léo Miolane, and Lenka Zdeborová. Optimal errors and phase transitions in high-dimensional generalized linear models. *Proceedings of the National Academy of Sciences of the United States of America*, 116(12):5451–5460, 2019.
- Mohsen Bayati and Andrea Montanari. The dynamics of message passing on dense graphs, with applications to compressed sensing. *IEEE Transactions on Information Theory*, 57(2):764–785, 2011.
- Eli Bingham, Jonathan P. Chen, Martin Jankowiak, Fritz Obermeyer, Neeraj Pradhan, Theofanis Karaletsos, Rohit Singh, Paul Szerlip, Paul Horsfall, and Noah D. Goodman. Pyro: Deep Universal Probabilistic Programming. *Journal of Machine Learning Research*, 2018.
- Christopher M. Bishop. *Pattern recognition and machine learning*. Springer, 2006.
- Christopher M. Bishop. Model-based machine learning. *Philosophical Transactions of the Royal Society A: Mathematical, Physical and Engineering Sciences*, 371(1984), 2013.
- Ashish Bora, Ajil Jalal, Eric Price, and Alexandros G Dimakis. Compressed sensing using generative models. In *Proceedings of the 34th International Conference on Machine Learning-Volume 70*, pages 537–546. JMLR.org, 2017.
- Burak Çakmak, Ole Winther, and Bernard H. Fleury. S-AMP: Approximate message passing for general matrix ensembles. *2014 IEEE Information Theory Workshop, ITW 2014*, 1(4):192–196, 2014.
- Burak Çakmak, Manfred Opper, Bernard H. Fleury, and Ole Winther. Self-Averaging Expectation Propagation. *arXiv*, 1608.06602, 2016.
- Bob Carpenter, Andrew Gelman, Matthew D. Hoffman, Daniel Lee, Ben Goodrich, Michael Betancourt, Marcus A. Brubaker, Jiqiang Guo, Peter Li, and Allen Riddell. Stan: A probabilistic programming language. *Journal of Statistical Software*, 76(1), 2017.
- Taco S. Cohen and Max Welling. Harmonic exponential families on manifolds. *32nd International Conference on Machine Learning, ICML 2015*, 3:1757–1765, 2015.
- Lehel Csató, Manfred Opper, and Ole Winther. Tap gibbs free energy, belief propagation and sparsity. In *Advances in Neural Information Processing Systems*, pages 657–663, 2002.
- A. P. Dempster, N. M. Laird, and D. B. Rubin. Maximum Likelihood from Incomplete Data Via the EM Algorithm . *Journal of the Royal Statistical Society: Series B (Methodological)*, 1977.

- Yash Deshpande and Andrea Montanari. Information-theoretically optimal sparse pca. In *2014 IEEE International Symposium on Information Theory*, pages 2197–2201. IEEE, 2014.
- Mohamad Dia, Nicolas Macris, Florent Krzakala, Thibault Lesieur, Lenka Zdeborová, et al. Mutual information for symmetric rank-one matrix estimation: A proof of the replica formula. In *Advances in Neural Information Processing Systems*, pages 424–432, 2016.
- David L. Donoho, Arian Maleki, and Andrea Montanari. Message-passing algorithms for compressed sensing. *Proceedings of the National Academy of Sciences of the United States of America*, 106(45):18914–18919, 2009.
- Alyson K Fletcher, Sundeep Rangan, and Philip Schniter. Inference in Deep Networks in High Dimensions. In *IEEE International Symposium on Information Theory*, 2018.
- Marylou Gabrié, Andre Manoel, Clément Luneau, Jean Barbier, Nicolas Macris, Florent Krzakala, and Lenka Zdeborová. Entropy and mutual information in models of deep neural networks. In *Advances in Neural Information Processing Systems 31*, 2018.
- Hong Ge, Kai Xu, and Zoubin Ghahramani. Turing: A language for flexible probabilistic inference. In *International Conference on Artificial Intelligence and Statistics, AISTATS 2018*, volume 84, 2018.
- Cédric Gerbelot, Alia Abbata, and Florent Krzakala. Asymptotic errors for convex penalized linear regression beyond gaussian matrices. *arXiv preprint arXiv:2002.04372*, 2020.
- Noah D. Goodman, Vikash K. Mansinghka, Daniel Roy, Keith Bonawitz, and Joshua B. Tenenbaum. Church: A language for generative models. In *Proceedings of the 24th Conference on Uncertainty in Artificial Intelligence, UAI 2008*, pages 220–229, 2008. ISBN 0974903949.
- Dongning Guo, Shlomo Shamai, and Sergio Verdú. Mutual information and minimum mean-square error in Gaussian channels. *IEEE Transactions on Information Theory*, 51(4):1261–1282, 2005.
- Tom Heskes and Onno Zoeter. Expectation Propagation for approximate inference in dynamic Bayesian networks. In *Proceedings UAI-2002*, pages 216–233, 2002.
- Tom Heskes, Manfred Opper, Wim Wiegerinck, Ole Winther, and Onno Zoeter. Approximate inference techniques with expectation constraints. *Journal of Statistical Mechanics: Theory and Experiment*, 11:277–300, 2005.
- Yoshiyuki Kabashima. A cdma multiuser detection algorithm on the basis of belief propagation. *Journal of Physics A: Mathematical and General*, 36(43):11111, 2003.
- Keras-VAE. Example of vae on mnist dataset using mlp. https://keras.io/examples/variational_autoencoder/.
- Florent Krzakala, Marc Mézard, Francois Sausset, Yifan Sun, and Lenka Zdeborová. Probabilistic reconstruction in compressed sensing: Algorithms, phase diagrams, and threshold achieving matrices. *Journal of Statistical Mechanics: Theory and Experiment*, 2012(8), 2012.
- Florent Krzakala, Andre Manoel, Eric W Tramel, and Lenka Zdeborová. Variational free energies for compressed sensing. In *2014 IEEE International Symposium on Information Theory*, pages 1499–1503. IEEE, 2014.
- Frank R. Kschischang, Brendan J. Frey, and Hans Andrea Loeliger. Factor graphs and the sum-product algorithm. *IEEE Transactions on Information Theory*, 47(2):498–519, 2001.
- Thibault Lesieur, Florent Krzakala, and Lenka Zdeborová. Constrained low-rank matrix estimation: Phase transitions, approximate message passing and applications. *Journal of Statistical Mechanics: Theory and Experiment*, 2017(7), 2017.
- Junjie Ma and Li Ping. Orthogonal amp. *IEEE Access*, 5:2020–2033, 2017.

- Antoine Maillard, Laura Foini, Alejandro Lage Castellanos, Florent Krzakala, Marc Mézard, and Lenka Zdeborová. High-temperature expansions and message passing algorithms. *Journal of Statistical Mechanics: Theory and Experiment*, 2019(11):113301, 2019.
- Andre Manoel, Florent Krzakala, Marc Mezard, and Lenka Zdeborova. Multi-layer generalized linear estimation. In *IEEE International Symposium on Information Theory*, 2017.
- Andre Manoel, Florent Krzakala, Gaël Varoquaux, Bertrand Thirion, and Lenka Zdeborová. Approximate message-passing for convex optimization with non-separable penalties. *arXiv*, 1809.06304, 2018.
- Christopher A Metzler, Arian Maleki, and Richard G Baraniuk. Optimal recovery from compressive measurements via denoising-based approximate message passing. In *2015 International Conference on Sampling Theory and Applications (SampTA)*, pages 508–512. IEEE, 2015.
- Marc Mezard and Andrea Montanari. *Information, physics, and computation*. Oxford University Press, 2009.
- Marc Mézard, Giorgio Parisi, and Miguel Virasoro. *Spin glass theory and beyond: An Introduction to the Replica Method and Its Applications*, volume 9. World Scientific Publishing Company, 1987.
- T. Minka, J.M. Winn, J.P. Guiver, Y. Zaykov, D. Fabian, and J. Bronskill. /Infer.NET 0.3, 2018. Microsoft Research Cambridge. <http://dotnet.github.io/infer>.
- Thomas P Minka. Expectation Propagation for approximate Bayesian inference. In *Proceedings of the UAI*, 2001a.
- Thomas P Minka. The EP energy function and minimization schemes, 2001b. URL <https://tminka.github.io/papers/ep/minka-ep-energy.pdf>.
- Manfred Opper and Ole Winther. Gaussian processes for classification: Mean-field algorithms. *Neural Computation*, 12:2655–2684, 2000.
- Manfred Opper and Ole Winther. Expectation consistent approximate inference. *Journal of Machine Learning Research*, 6:2177–2206, 2005a.
- Manfred Opper and Ole Winther. Expectation consistent free energies for approximate inference. *Advances in Neural Information Processing Systems*, 17:1001–1008, 2005b.
- Neal Parikh and Stephen Boyd. Proximal Algorithms. *Foundations and Trends in Optimization*, 1(3):127–239, 2014. doi: 10.1561/24000000003.
- Giorgio Parisi and Marc Potters. Mean-field equations for spin models with orthogonal interaction matrices. *Journal of Physics A: Mathematical and General*, 28(18):5267, 1995.
- Judea Pearl. *Probabilistic Reasoning in Intelligent Systems: Networks of Plausible Inference*. Morgan Kaufmann Publishers Inc., San Francisco, CA, USA, 1988. ISBN 0934613737.
- F. Pedregosa, G. Varoquaux, A. Gramfort, V. Michel, B. Thirion, O. Grisel, M. Blondel, P. Prettenhofer, R. Weiss, V. Dubourg, J. Vanderplas, A. Passos, D. Cournapeau, M. Brucher, M. Perrot, and E. Duchesnay. Scikit-learn: Machine learning in Python. *Journal of Machine Learning Research*, 12:2825–2830, 2011.
- Amelia Perry, Alexander S. Wein, Afonso S. Bandeira, and Ankur Moitra. Message-Passing Algorithms for Synchronization Problems over Compact Groups. *Communications on Pure and Applied Mathematics*, 71(11):2275–2322, 2018.
- Sundee Rangan. Generalized approximate message passing for estimation with random linear mixing. In *2011 IEEE International Symposium on Information Theory Proceedings*, pages 2168–2172. IEEE, 2011.
- Sundee Rangan and Alyson K Fletcher. Iterative estimation of constrained rank-one matrices in noise. In *2012 IEEE International Symposium on Information Theory Proceedings*, pages 1246–1250. IEEE, 2012.

- Sundeeep Rangan, Philip Schniter, and Alyson K Fletcher. Vector approximate message passing. In *IEEE International Symposium on Information Theory - Proceedings*, pages 1588–1592, 2017.
- Carl Edward Rasmussen and Christopher K. I. Williams. *Gaussian Processes for Machine Learning*. MIT Press, 2006.
- Galen Reeves. Additivity of Information in Multilayer Networks via Additive Gaussian Noise Transforms. *arXiv*, 1710.04580v1, 2017.
- Galen Reeves and Henry D. Pfister. The replica-symmetric prediction for compressed sensing with Gaussian matrices is exact. In *IEEE International Symposium on Information Theory - Proceedings*, 2016.
- John Salvatier, Thomas Wiecki, and Christopher Fonnesbeck. Probabilistic programming in python using pymc3. 01 2016. doi: 10.7287/PEERJ.PREPRINTS.1686V1.
- Philip Schniter, Sundeeep Rangan, and Alyson K Fletcher. Vector approximate message passing for the generalized linear model. In *Conference Record - Asilomar Conference on Signals, Systems and Computers*, pages 1525–1529, 2017.
- Jacob Schreiber. pomegranate: Fast and flexible probabilistic modeling in python. *Journal of Machine Learning Research*, 18:1–6, 2018.
- Takashi Shinzato and Yoshiyuki Kabashima. Learning from correlated patterns by simple perceptrons. *Journal of Physics A: Mathematical and Theoretical*, 42(1):015005, 2008a.
- Takashi Shinzato and Yoshiyuki Kabashima. Perceptron capacity revisited: classification ability for correlated patterns. *Journal of Physics A: Mathematical and Theoretical*, 41(32):324013, 2008b.
- Subhojit Som and Philip Schniter. Compressive imaging using approximate message passing and a markov-tree prior. *IEEE transactions on signal processing*, 60(7):3439–3448, 2012.
- Jin Tan, Yanting Ma, and Dror Baron. Compressive imaging via approximate message passing with image denoising. *IEEE Transactions on Signal Processing*, 63(8):2085–2092, 2015.
- Dustin Tran, Alp Kucukelbir, Adji B. Dieng, Maja Rudolph, Dawen Liang, and David M. Blei. Edward: A library for probabilistic modeling, inference, and criticism. *arXiv 1610.09787*, 2016.
- Antonia M. Tulino and Sergio Verdú. *Random matrix theory and wireless communications*. 2004.
- Jeremy Vila, Philip Schniter, Sundeeep Rangan, Florent Krzakala, and Lenka Zdeborova. Adaptive damping and mean removal for the generalized approximate message passing algorithm. *ICASSP, IEEE International Conference on Acoustics, Speech and Signal Processing - Proceedings*, pages 2021–2025, 2015.
- Martin J. Wainwright and Michael I. Jordan. *Graphical models, exponential families, and variational inference*. 2008.
- Frank Wood, Jan Willem Van De Meent, and Vikash Mansinghka. A new approach to probabilistic programming inference. *Journal of Machine Learning Research*, 33:1024–1032, 2014.
- Jonathan S. Yedidia, William T. Freeman, and Yair Weiss. Constructing free-energy approximations and generalized belief propagation algorithms. *IEEE Transactions on Information Theory*, 51(7):2282–2312, 2005.
- JS Yedidia and WT Freeman. Understanding belief propagation and its generalizations. *Exploring artificial intelligence in the new millennium*, pages 239 – 269, 2001.
- Lenka Zdeborová and Florent Krzakala. Statistical physics of inference: thresholds and algorithms. *Advances in Physics*, 65(5):453–552, 2016.
- Onno Zoeter and Tom Heskes. Change point problems in linear dynamical systems. *Journal of Machine Learning Research*, 6:1999–2026, 2005.